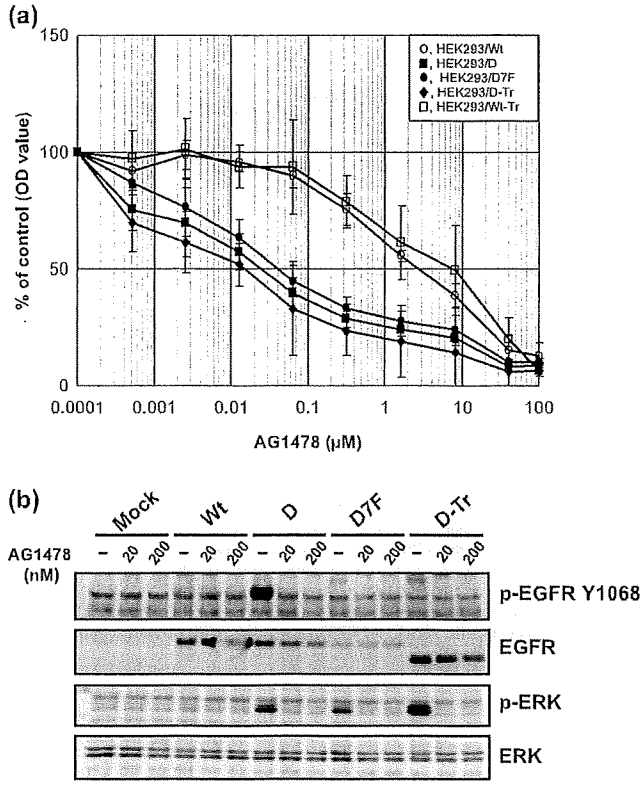

Fig. 3. Sensitivity of cell growth and downstream epidermal growth factor receptor (EGFR) signaling to AG1478 in the mutant EGFR transfectants. (a) The growth-inhibitory effect of AG1478 in HEK293/Wt, HEK293/Wt-Tr, HEK293/D, HEK293/D7F, and HEK293/D-Tr cells. The seeded cells were exposed to AG1478 for 72 h and the cellular proliferative activity was determined by MTT assay. (b) The HEK293/Wt, HEK293/D, HEK293/D7F, and HEK293/D-Tr cells were incubated in 1% serum starve medium for 12 h, followed by exposure to 20 or 200 nM AG1478 for 3 h at 37°C. The cell lysates were immunoblotted with anti-phospho-EGFR (p-EGFR Y1068), anti-EGFR (recognizing the extracellular domain), anti-phospho-ERK, or anti-ERK antibodies. Mock, HEK293/Mock; Wt, HEK293/Wt; Wt-Tr, HEK293/Wt-Tr; D, HEK293/D; D7F, HEK293/D7F; D-Tr, HEK293/D-Tr.

EGFR lacking C-terminal autophosphorylation sites with endogenous HER receptors contributes to the signal transduction. It is thus speculated that homodimerization of EGFR lacking C-terminal autophosphorylation sites transduces the signals to downstream molecules. Indeed, the results of the chemical crosslinking assay revealed clear homodimerized bands in the HEK293/Wt, HEK293/D, and HEK293/D7F cells (Fig. 5a). In the HEK293/D-Tr cells, homodimerized bands with lower molecular weights (indicated by the black arrow) were detected (Fig. 5a) and these dimers were not phosphorylated (Fig. 5b). Taken together, we speculate that EGFR lacking C-terminal autophosphorylation sites form homodimers.

Despite a lack of C-terminal autophosphorylation sites, transfected cells retain their capacity for EGFR-dependent Shc phosphorylation. Binding of adaptor proteins to the C-terminal region of EGFR is essential for EGFR signal transduction. It is widely recognized that tyrosines 1068 and 1086 are most important for Sos and Grb2 activation; EGFR-D7F and EGFR-D-Tr lack these tyrosine residues. Sos and Grb2 were coprecipitated with EGFR in the HEK293/Wt and HEK293/D cells, but not in the HEK293/D7F or HEK293/D-Tr cells (Fig. 6a). The bands were confirmed by reblotting of the membranes used for immunoblotting (data not shown). Another adaptor protein, Shc, also binds to the C-terminal region of EGFR, and phosphorylation of Shc activates the ERK pathway. An increase in phosphorylated p46 and p52 Shc was observed in the HEK293/D, HEK293/D7F, and HEK293/D-Tr cells compared with the HEK293/Mock and HEK/Wt cells (Fig. 6b). The phosphorylation of Shc observed in the HEK293/D, HEK293/D7F, and HEK293/D-Tr cells was completely inhibited by 20 nM AG1478 (Fig. 6c). These results suggest that EGFR lacking C-terminal autophosphorylation sites activates Shc in a C-terminal-independent manner, and that Shc-mediated signals may be involved in the hypersensitivity to EGFR TKI of HEK293 cells expressing EGFR lacking C-terminal autophosphorylation sites.

Discussion

In the present study, we investigated the relationship between phosphorylation of tyrosine residues in the C-terminal region of EGFR and cellular sensitivity to EGFR TKI. Increased phosphorylation of Shc and ERK was observed in HEK293/D7F and HEK293/D-Tr cells, which expressed EGFR lacking autophosphorylation sites in the C-terminal region. Previous reports have demonstrated

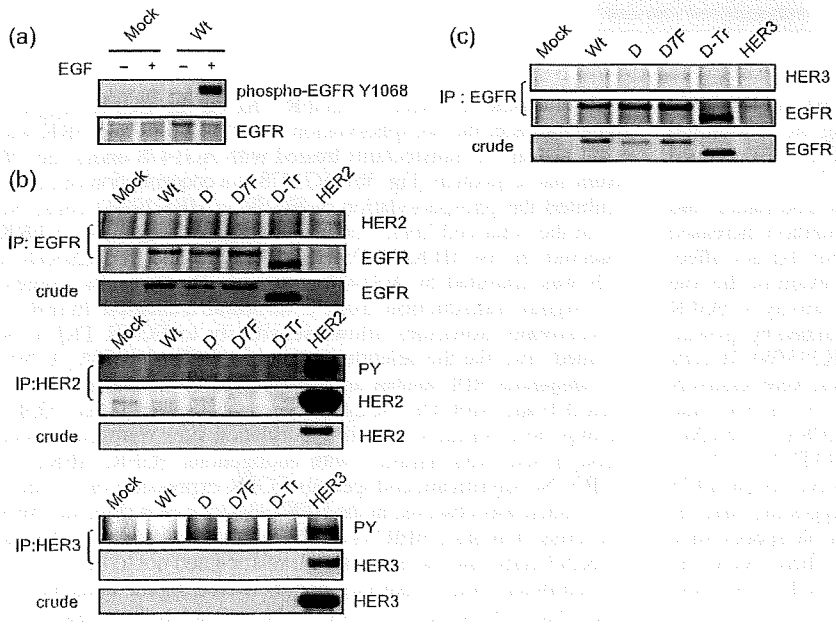

Fig. 4. Heterodimerization of mutant epidermal growth factor receptor (EGFR) with endogenous receptors of the HER family in mutant EGFR transfectants. Expression of endogenous EGFR and response to epidermal growth factor stimulation. HEK293/Mock, HEK293/Wt, HEK293/D, HEK293/D7F, and HEK293/D-Tr cells were incubated in 1% serum starve medium for 12 h followed by the addition of 10 ng/mL epidermal growth factor for 10 min at 37°C. (a) The whole-cell lysates of HEK293/Mock and HEK293/W+ cells containing equal amounts of protein were immunoblotted with anti-phospho-EGFR (p-EGFR Y1068) and anti-EGFR (recognized extracellular domain). (b,c) The lysates were immunoprecipitated with anti-EGFR, anti-HER2, or anti-HER3 antibodies, and immunoblotted with anti-EGFR, anti-HER2, anti-HER3, or anti-phosphotyrosine antibodies to detect the dimerization and phosphorylation of EGFR and endogenous HER2 or HER3. HER2, HER2-introduced HEK293 cells as a positive control; HER3, HER3-introduced HEK293 cells as a positive control.

doi: 10.1111/j.1349-7006.2008.01071.x

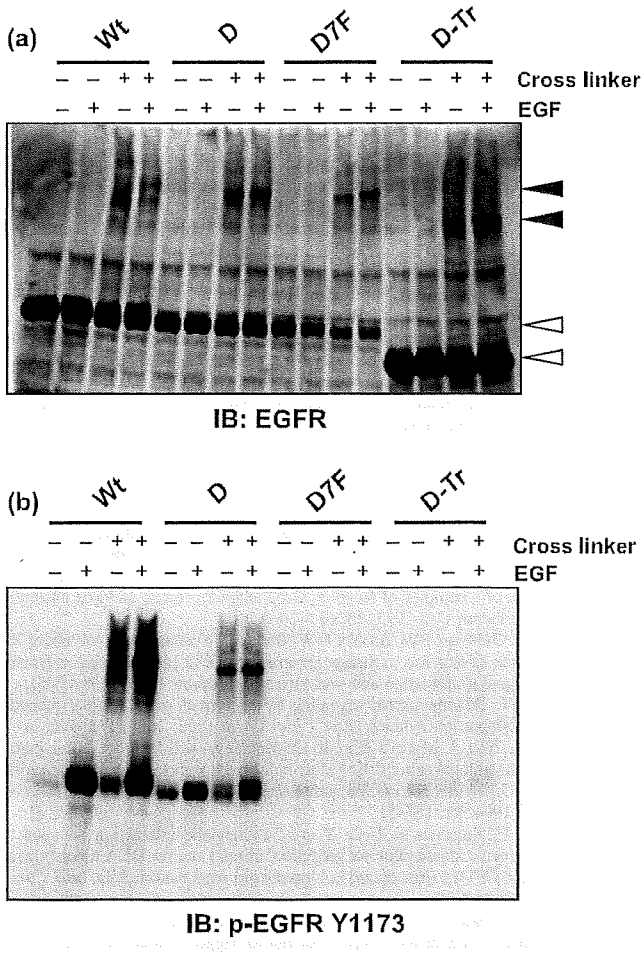

Fig. 5. The cells under 1% serum starved medium were allowed to react with 2 mM of the chemical crosslinking regent BS_3 before the crosslinking reaction was quenched. The cell lysates were immunoblotted with (a) anti-epidermal growth factor receptor (EGFR) (recognizing the extracellular domain) and (b) anti-phosphoEGFR (p-EGFR Y1173) antibodies to detect the dimerization and phosphorylation of wild-type and mutant EGFR. Black arrow, EGFR dimer; open arrow, EGFR monomer. Mock, HEK293/Mock; Wt, HEK293/Wt; D, HEK 293/D; D7F, HEK293/D7F; D-Tr, HEK293/D-Tr. EGF, epidermal growth factor.

that cells expressing EGFR lacking C-terminal autophospholylation sites retain EGF-induced mitogenic and transforming activity.[27,28] Our data and these previous reports suggest that there exist other EGFR signaling pathways besides those mediated by the C-terminal tyrosine residues. In addition, these signaling pathways are operative in the active EGFR mutant (delE746_A750) as well as wild-type EGFR.[28] The results of our growth-inhibition assay demonstrated the hypersensitivity of HEK293/D7F and HEK293/D-Tr cells to EGFR TKI, and phosphorylation of ERK and Shc in these cells was also inhibited. These results suggest that this EGFR signaling pathway contributes to tumor cell growth.

We demonstrated the hypersensitivity of the transfectants (HEK293/D7F and HEK293/D-Tr cells) to AG1478. We previously reported the hypersensitivity of transfectants carrying mutant EGFR to AG1478 as well as gefitinib, ZD6474, and erlotinib.[8,15,31] Therefore, it can be easily speculated that the HEK293/D7F and HEK293/D-Tr cells would also be hypersensitive to the clinically available EGFR TKI and AG1478.

Somatic EGFR mutation in lung cancer has been reported, and over 20 types of mutations have been reported.[10] The L858R point mutation in exon 21 of EGFR is a major point mutation (such as in delE746_A750) that contributes to EGFR TKI hypersensitivity.[32] Interestingly, we constructed cells that overexpressed EGFR-Wt-Tr and EGFR-D-Tr, and a mutant truncated form of EGFR similar to EGFR-Wt-Tr was previously found in patients with glioblastoma.[33] The mutant was truncated at amino acid 958 of EGFR and the frequency was relatively high in 7 of 48 patients. Therefore, it would be of interest to determine in future studies whether this C-terminal-truncated form of delE746_A750 EGFR, similar to EGFR-D-Tr, might be identifiable in human materials in the clinical setting.

We attempted to clarify the signaling pathway from the C-terminal region of EGFR. We observed the phosphorylation of ERK and Shc in HEK293/D7F and HEK293/D-Tr cells, and these phosphorylations were inhibited by exposure to AG1478. These phosphorylations were not observed in HEK293/Mock, HEK293/Wt, or HEK293/Wt-Tr cells. Our results suggest that the constitutively active mutant EGFR lacking C-terminal autophosphorylation sites is sufficient for activation of the downstream pathway. However, it remains unknown how signals are transduced from EGFR without a C-terminal region to Shc, as no direct binding of Grb2 or Shc with EGFR lacking the C-terminal region was detected in the HEK293/D7F and HEK293/D-Tr cells (Fig. 6a). We attempted to identify the mediator molecules binding to EGFR-D-Tr and EGFR-D7F by mass analysis of immunoprecipitates; however, no clear mediator molecules were identified. As a possible indirect mechanism, Sasaoka *et al.* postulated that ErbB2–Shc signals from EGFR lacking C-terminal autophosphorylation sites.[34] However, we consider this unlikely from the results of our experiments because no significant expression of Erb2 was detected in the HER293 cells.

The results of the crosslinking assay demonstrated that a complex of lower molecular weight was present in the HEK293/D-Tr cells compared with the HER293/Wt cells, indicating that truncated EGFR forms homodimers in the HEK293/D-Tr cells. Thus, it can be speculated that homodimerized truncated EGFR directly transduces signals downstream.

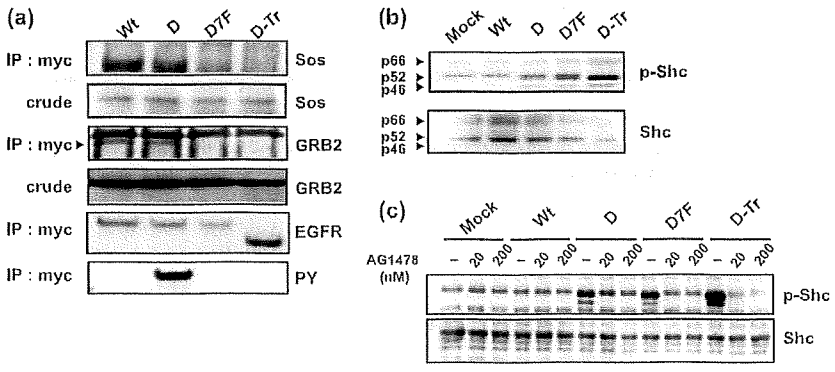

Fig. 6. Interaction between mutant epidermal growth factor receptor (EGFR) and adaptor proteins. The cells were cultured under normal conditions. (a) The lysates of HEK293/Wt, HEK293/D, HEK293/D7F, and HEK293/D-Tr cells were immunoprecipitated with anti-myc tag antibody; the precipitates were immunoblotted with anti-son of sevenless homolog (Sos) and anti-growth factor receptor-bound protein (Grb) 2 antibodies. (b) Whole-cell lysates containing equal amounts of protein were immunoblotted with anti-phospho-Src homology and collagen homology (Shc) and anti-Shc antibodies. (c) The cells incubated in 1% serum starve medium for 12 h were treated with 20 or 200 nM AG1478 for 3 h and then the lysates were immunoblotted with anti-phospho-Shc or anti-Shc antibodies. Mock, HEK293/Mock; Wt, HEK293/Wt; D, HEK293/D; D7F, HEK293/D7F; D-Tr, HEK293/D-Tr. PY, anti-phospho-tyrosine.

In conclusion, our results indicate that an as-yet-unknown signaling pathway of EGFR exists that is independent of the C-terminal region of EGFR, and these regions are not required for cellular sensitivity to EGFR TKI.

Acknowledgments

This work was supported by a research grant from the Third Term Comprehensive 10-Year Strategy for Cancer Control.

References

1 Gusterson B, Cowley G, McIlhinney J, Ozanne B, Fisher C, Reeves B. Evidence for increased epidermal growth factor receptors in human sarcomas. *Int J Cancer* 1985; **36**: 689–93.
2 Bargmann CI, Hung MC, Weinberg RA. The *neu* oncogene encodes an epidermal growth factor receptor-related protein. *Nature* 1986; **319**: 226–30.
3 Cowley GP, Smith JA, Gusterson BA. Increased EGF receptors on human squamous carcinoma cell lines. *Br J Cancer* 1986; **53**: 223–9.
4 Mendelsohn J, Baselga J. Epidermal growth factor receptor targeting in cancer. *Semin Oncol* 2006; **33**: 369–85.
5 Karamouzis MV, Grandis JR, Argiris A. Therapies directed against epidermal growth factor receptor in aerodigestive carcinomas. *JAMA* 2007; **298**: 70–82.
6 Rocha-Lima CM, Soares HP, Raez LE, Singal R. EGFR targeting of solid tumors. *Cancer Control* 2007; **14**: 295–304.
7 Paez JG, Janne PA, Lee JC *et al.* EGFR mutations in lung cancer: correlation with clinical response to gefitinib therapy. *Science* 2004; **304**: 1497–500.
8 Lynch TJ, Bell DW, Sordella R *et al.* Activating mutations in the epidermal growth factor receptor underlying responsiveness of non-small-cell lung cancer to gefitinib. *N Engl J Med* 2004; **350**: 2129–39.
9 Amann J, Kalyankrishna S, Massion PP *et al.* Aberrant epidermal growth factor receptor signaling and enhanced sensitivity to EGFR inhibitors in lung cancer. *Cancer Res* 2005; **65**: 226–35.
10 Mitsudomi T, Yatabe Y. Mutations of the epidermal growth factor receptor gene and related genes as determinants of epidermal growth factor receptor tyrosine kinase inhibitors sensitivity in lung cancer. *Cancer Sci* 2007; **98**: 1817–24.
11 Riely GJ, Pao W, Pham D *et al.* Clinical course of patients with non-small cell lung cancer and epidermal growth factor receptor exon 19 and exon 21 mutations treated with gefitinib or erlotinib. *Clin Cancer Res* 2006; **12**: 839–44.
12 Arao T, Fukumoto H, Takeda M, Tamura T, Saijo N, Nishio K. Small in-frame deletion in the epidermal growth factor receptor as a target for ZD6474. *Cancer Res* 2004; **64**: 9101–4.
13 Koizumi F, Shimoyama T, Taguchi F, Saijo N, Nishio K. Establishment of a human non-small cell lung cancer cell line resistant to gefitinib. *Int J Cancer* 2005; **116**: 36–44.
14 Naruse I, Ohmori T, Ao Y *et al.* Antitumor activity of the selective epidermal growth factor receptor-tyrosine kinase inhibitor (EGFR-TKI) Iressa (ZD1839) in an EGFR-expressing multidrug-resistant cell line *in vitro* and *in vivo*. *Int J Cancer* 2002; **98**: 310–15.
15 Sakai K, Arao T, Shimoyama T *et al.* Dimerization and the signal transduction pathway of a small in-frame deletion in the epidermal growth factor receptor. *FASEB J* 2006; **20**: 311–13.
16 Sakai K, Yokote H, Murakami-Murofushi K, Tamura T, Saijo N, Nishio K. In-frame deletion in the EGF receptor alters kinase inhibition by gefitinib. *Biochem J* 2006; **397**: 537–43.
17 Olayioye MA, Neve RM, Lane HA, Hynes NE. The ErbB signaling network: receptor heterodimerization in development and cancer. *EMBO J* 2000; **19**: 3159–67.
18 Yarden Y, Sliwkowski MX. Untangling the ErbB signalling network. *Nat Rev Mol Cell Biol* 2001; **2**: 127–37.
19 Batzer AG, Blaikie P, Nelson K, Schlessinger J, Margolis B. The phosphotyrosine interaction domain of Shc binds an LXNPXY motif on the epidermal growth factor receptor. *Mol Cell Biol* 1995; **15**: 4403–9.
20 Batzer AG, Rotin D, Urena JM, Skolnik EY, Schlessinger J. Hierarchy of binding sites for Grb2 and Shc on the epidermal growth factor receptor. *Mol Cell Biol* 1994; **14**: 5192–201.
21 Ono M, Hirata A, Kometani T *et al.* Sensitivity to gefitinib (Iressa, ZD1839) in non-small cell lung cancer cell lines correlates with dependence on the epidermal growth factor (EGF) receptor/extracellular signal-regulated kinase 1/2 and EGF receptor/Akt pathway for proliferation. *Mol Cancer Ther* 2004; **3**: 465–72.
22 Quesnelle KM, Boehm AL, Grandis JR. STAT-mediated EGFR signaling in cancer. *J Cell Biochem* 2007; **102**: 311–19.
23 Ravichandran KS, Lorenz U, Shoelson SE, Burakoff SJ. Interaction of Shc with Grb2 regulates association of Grb2 with mSOS. *Mol Cell Biol* 1995; **15**: 593–600.
24 Rubio I, Rennert K, Wittig U *et al.* Ras activation in response to phorbol ester proceeds independently of the EGFR via an unconventional nucleotide-exchange factor system in COS-7 cells. *Biochem J* 2006; **398**: 243–56.
25 Buday L, Downward J. Epidermal growth factor regulates p21ras through the formation of a complex of receptor, Grb2 adapter protein, and Sos nucleotide exchange factor. *Cell* 1993; **73**: 611–20.
26 Egan SE, Giddings BW, Brooks MW, Buday L, Sizeland AM, Weinberg RA. Association of Sos Ras exchange protein with Grb2 is implicated in tyrosine kinase signal transduction and transformation. *Nature* 1993; **363**: 45–51.
27 Decker SJ. Transmembrane signaling by epidermal growth factor receptors lacking autophosphorylation sites. *J Biol Chem* 1993; **268**: 9176–9.
28 Gotoh N, Tojo A, Muroya K *et al.* Epidermal growth factor-receptor mutant lacking the autophosphorylation sites induces phosphorylation of Shc protein and Shc-Grb2/ASH association and retains mitogenic activity. *Proc Natl Acad Sci USA* 1994; **91**: 167–71.
29 Koizumi F, Kanzawa F, Ueda Y *et al.* Synergistic interaction between the EGFR tyrosine kinase inhibitor gefitinib ('Iressa') and the DNA topoisomerase I inhibitor CPT-11 (irinotecan) in human colorectal cancer cells. *Int J Cancer* 2004; **108**: 464–72.
30 Yoshida T, Okamoto I, Okabe T *et al.* Matuzumab and cetuximab activate the epidermal growth factor receptor but fail to trigger downstream signaling by Akt or Erk. *Int J Cancer* 2008; **122**: 1530–8.
31 Arao T, Yanagihara K, Takigahira M *et al.* ZD6474 inhibits tumor growth and intraperitoneal dissemination in a highly metastatic orthotopic gastric cancer model. *Int J Cancer* 2006; **118**: 483–9.
32 Mitsudomi T, Kosaka T, Endoh H *et al.* Mutations of the epidermal growth factor receptor gene predict prolonged survival after gefitinib treatment in patients with non-small-cell lung cancer with postoperative recurrence. *J Clin Oncol* 2005; **23**: 2513–20.
33 Frederick L, Wang XY, Eley G, James CD. Diversity and frequency of epidermal growth factor receptor mutations in human glioblastomas. *Cancer Res* 2000; **60**: 1383–7.
34 Sasaoka T, Langlois WJ, Bai F *et al.* Involvement of ErbB2 in the signaling pathway leading to cell cycle progression from a truncated epidermal growth factor receptor lacking the C-terminal autophosphorylation sites. *J Biol Chem* 1996; **271**: 8338–44.

Supporting Information

Additional Supporting Information may be found in the online version of this article:

Table S1. Primer set for epidermal growth factor receptor cDNA with substitution of seven tyrosine residues to phenylalanine in the C-terminal region

Please note: Wiley-Blackwell are not responsible for the content or functionality of any supporting materials supplied by the authors. Any queries (other than missing material) should be directed to the corresponding author for the article.

doi: 10.1111/j.1349-7006.2008.01071.x

the FEBS Journal

Mitogen-activated protein kinase phosphatase-1 modulated JNK activation is critical for apoptosis induced by inhibitor of epidermal growth factor receptor-tyrosine kinase

Kenji Takeuchi[1], Tomohiro Shin-ya[1], Kazuto Nishio[2] and Fumiaki Ito[1]

1 Department of Biochemistry, Faculty of Pharmaceutical Sciences, Setsunan University, Osaka, Japan
2 Department of Genome Biology, Kinki University School of Medicine, Osaka, Japan

Keywords
AG1478; c-Jun N-terminal kinase; epidermal growth factor receptor; mitogen-activated protein kinase phosphatase-1; non-small-cell lung cancer

Correspondence
K. Takeuchi, Department of Biochemistry, Faculty of Pharmaceutical Sciences, Setsunan University, Hirakata, Osaka 573-0101, Japan
Fax: +81 72 866 3117
Tel: +81 72 866 3118
E-mail: takeuchi@pharm.setsunan.ac.jp

(Received 29 August 2008, revised 6 December 2008, accepted 16 December 2008)

doi:10.1111/j.1742-4658.2008.06861.x

Alterations resulting in enhanced epidermal growth factor receptor (EGFR) expression or function have been documented in a variety of tumors. Therefore, EGFR-tyrosine kinase is a promising therapeutic target. Although *in vitro* and *in vivo* studies have shown the anti-tumor activity of EGFR-tyrosine kinase inhibitors against various tumor types, little is known about the mechanism by which such inhibitors effect their anti-tumor action. AG1478 is known to selectively inhibit EGFR-tyrosine kinase. In this study, we showed that AG1478 caused apoptosis and apoptosis-related reactions such as the activation of caspase 3 in human non-small cell lung cancer cell line PC-9. To investigate the signaling route by which AG1478 induced apoptosis, we examined the activation of c-Jun N-terminal kinase (JNK) and mitogen-activated protein kinase p38 in AG1478-treated PC-9 cells. JNK, but not p38, was significantly activated by AG1478 as determined by both immunoblot analysis for levels of phosphorylated JNK and an *in vitro* activity assay. Various types of stimuli activated JNK through phosphorylation by the dual-specificity JNK kinases, but the dual-specificity JNK kinases MKK4 and MKK7 were not activated by AG1478 treatment. However, JNK phosphatase, i.e. mitogen-activated protein kinase phosphatase-1 (MKP-1), was constitutively expressed in the PC-9 cells, and its expression level was reduced by AG1478. The inhibition of JNK activation by ectopic expression of MKP-1 or a dominant-negative form of JNK strongly suppressed AG1478-induced apoptosis. These results reveal that JNK, which is activated through the decrease in the MKP-1 level, is critical for EGFR-tyrosine kinase inhibitor-induced apoptosis.

Epidermal growth factor receptor (EGFR), a member of the ErbB family, is important in the regulation of growth, differentiation and survival of various cell types. Ligand binding to EGFR results in receptor dimerization, activation of its tyrosine kinase and phosphorylation of its C-terminal tyrosine residues. The tyrosine-phosphorylated motifs of EGFR recruit various adaptors or signaling molecules [1,2]. EGFR is able to activate a variety of signaling pathways through its association with these molecules. The mitogen-activated protein kinase (MAPK) pathway leading to phosphorylation of extracellular signal-regulated

Abbreviations
EGFR, epidermal growth factor receptor; ERK, extracellular signal-regulated kinase; JNK, c-Jun N-terminal kinase; MAPK, mitogen-activated protein kinase; MKP-1, mitogen-activated protein kinase phosphatase-1; NSCLC, non-small-cell lung cancer; PI, propidium iodide; PtdIns3-K, phosphatidylinositol 3-kinase; SAPK, stress-activated MAPK.

kinase (ERK) 1/2 plays an essential role in EGF-induced cell growth; and the phosphatidylinositol 3-kinase (PtdIns3K) pathway is also important for cell growth and cell survival. One way by which PtdIns3K signals cells to survive is by activating protein kinase PDK1 which in turn phosphorylates Akt.

EGFR gene mutations or EGFR gene amplification is detected in various types of malignancy [1,2]; therefore, EGFR-tyrosine kinase is a promising therapeutic target. Orally active small molecules against EGFR (e.g. gefitinib and erlotinib) show evident anti-tumor effects in patients with various cancers, particularly non-small cell lung cancer (NSCLC) [3–5]. Beneficial responsiveness to EGFR-targeting chemicals in NSCLC patients is closely associated with EGFR mutations in the kinase domain [6–8].

The induction of apoptosis has been considered as a major mechanism for gefitinib-mediated anti-cancer effects [9,10]. Lung cancer cells harboring mutant EGFRs become dependent on them for their survival and, consequently, undergo apoptosis following inhibition of EGFR tyrosine kinase by gefitinib. Gefitinib has been shown to inhibit cell survival and growth signaling pathways such as the Ras-MAPK pathway and PtdIns3K/Akt pathway, as a consequence of inactivation of EGFR [10–13]. The PtdIns3K/Akt pathway is downregulated in response to gefitinib only in NSCLC cell lines that are growth-inhibited by gefitinib [14]. So, it is thought that the PtdIns3K/Akt pathway plays a critical role in the gefitinib-induced anti-tumor action. Furthermore, some reports have demonstrated that blockage of the EGFR activity with gefitinib is able to cause suppression of a downstream signaling pathway through Ras-MAPK and/or PtdIns3K/Akt, and induce apoptosis through activation of the pro-apoptotic Bcl-2 family protein Bad or Bax [9,15].

In mammals, three major groups of MAPK have been identified [16–18]. The c-Jun N-terminal kinase (JNK), also known as stress-activated MAPK (SAPK), represents a group of MAPKs that are activated by treatment of cells with cytokines or by exposure of cells to a variety of stresses [19–21]. JNK activity has been implicated in both apoptosis and survival signaling and is tightly controlled by both protein kinases and protein phosphatases [22–24]. Various types of stimuli activate JNK through phosphorylation by the dual-specificity kinase MKK4 or MKK7 [18,25]. By contrast, any types of stimuli can inactivate JNK through induction of the expression of JNK phosphatases, which include dual-specificity (threonine/tyrosine) phosphatases [26–28].

PC-9 cells are gefitinib-sensitive human NSCLC cell lines with a mutation (delE746-A750) in their EGFR, which allows the receptor to be autophosphorylated independent of EGF. In this study, we investigated the signaling route by which the EGFR tyrosine kinase inhibitor AG1478 induces apoptosis in PC-9 cells. There is a general agreement on the hypothesis that the inhibition of ERK1/2 MAPK and/or PtdIns3K/Akt growth/survival signaling cascades leads to apoptosis of cancer cells. However, there are no studies addressing the role of JNK in apoptosis induced by EGFR tyrosine kinase inhibitors. Here, we demonstrate that JNK-phosphatase MKP-1 expression is controlled by a signal downstream of EGFR and that if this signal is abolished by an inhibitor of EGFR tyrosine kinase, the decreased MKP-1 activity can result in JNK activation, leading to the induction of apoptosis.

Results

We first examined the effect of AG1478 on the viability of human NSCLC cell line PC-9. Treatment of the cells with AG1478 markedly suppressed the cell viability, as determined by the results of a colorimetric assay (Fig. 1A). Photographic observation of AG1478-treated PC-9 cells revealed that AG1478 decreased the percentage of adherent cells in a time-dependent manner (Fig. 1B). When AG1478-treated PC-9 cells were stained with Hoechst–propidium iodide (PI), cells with condensed chromatin and fragmented nuclei, which are characteristic of the nuclear changes in apoptotic cells, were seen in both adherent and non-adherent cell populations (data not shown). To confirm whether this AG1478-induced cell death resulted from apoptosis, we examined caspase 3 activity after exposing the cells to 500 nM AG1478. As shown in Fig. 1C, caspase 3 activity was increased in a time-dependent manner. It thus appears that AG1478 reduced the survival rate of PC-9 cells by activating the apoptotic pathway.

It is important to know how AG1478 affected the survival rate of PC-9 cells. Many studies have shown that enhanced JNK activity may be required for initiation of stress-induced apoptosis [29,30]. To examine whether JNK might be activated by AG1478, we treated PC-9 cells with AG1478 for various periods (Fig. 2A). Activation of JNK was measured by performing an immune complex kinase assay using bacterially expressed GST–c-Jun as a substrate. Phosphorylation of c-Jun appeared 1 h after AG1478 addition, with a maximum level at 24 h. We next determined the phosphorylation of JNK in the presence of AG1478. PC-9 cells were incubated with AG1478 for several periods, and cell lysates were prepared from these cells to determine the phosphorylation of JNK by immunoblotting (Fig. 2B). AG1478

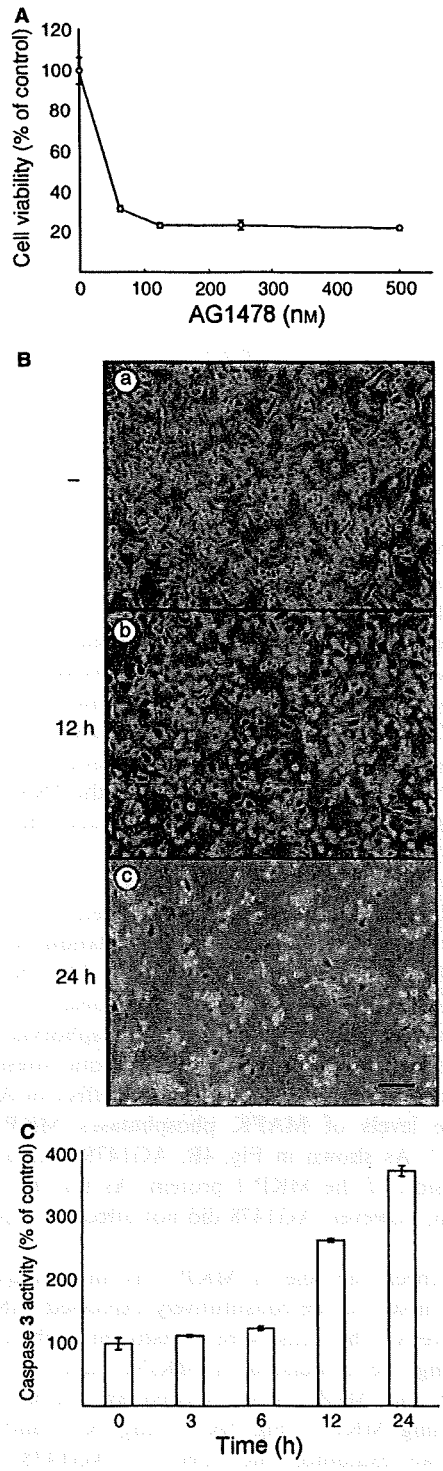

Fig. 1. Induction of apoptosis by AG1478. (A) PC-9 cells were seeded into a 96-well microplate, and treated with AG1478 at various concentrations for 48 h. The viability of cells was determined by conducting WST-8 assays. The value of untreated cells was considered as 100% viability. The data presented are the mean ± SD (n = 6). (B) PC-9 cells were seeded at a density 3×10^5 cells per 60 mm dish and then treated with 500 nM AG1478. The phase-contrast photomicrographs were taken 0 (a), 12 (b) or 24 h (c) after incubation with AG1478. Scale bar, 100 μm. (C) PC-9 cells were treated with 500 nM AG1478. Lysates were prepared at the indicated time points after the AG1478 addition and analyzed for caspase **3** activity by using a fluorometric substrate-based assay. Each point is the mean of triplicate samples, and the bar represents the standard deviation. Similar results were obtained from three separate experiments.

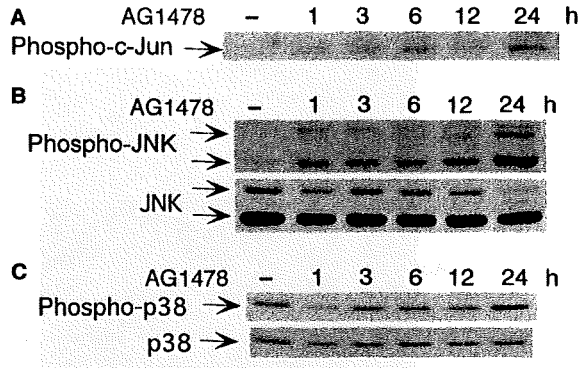

Fig. 2. JNK activation by AG1478. PC-9 cells were treated with 500 nM AG1478 and lysed on ice at the indicated time points. (A) JNK–c-Jun complexes were collected by glutathione *S*-transferase–c-Jun agarose beads and then assayed *in vitro* for kinase activity by using c-Jun as a substrate. The phospho-c-Jun product was detected by immunoblotting. (B) The cell lysates were normalized for protein content and analyzed for phospho-JNK content (upper), as well as for JNK content (lower). (C) The cell lysates were analyzed for phospho-p38 content (upper panel), as well as for p38 (lower). Similar results were obtained from three separate experiments.

intensively stimulated phosphorylation of JNK on its threonine 183 and tyrosine 185, and their phosphorylation levels continued to increase for at least 24 h. However, the activation of p38, another MAP kinase sub-family member, was not evident up to 12 h after AG1478 treatment; although an increase in the phosphorylation of p38 was detected at 24 h (Fig. 2C). Phosphorylation of ERK1/2, prototypical MAPK, was decreased by the treatment with AG1478 at the same time as activation of JNK (data not shown).

Neither SB203580 nor PD98059, inhibitors of p38 and ERK1/2, respectively, affected AG1478-induced apoptosis in PC-9 cells (data not shown), suggesting that neither p38 nor ERK1/2 mainly transmit the apoptotic signal of AG1478 in the PC-9 cells. If JNK plays an important role in AG1478-induced apoptosis,

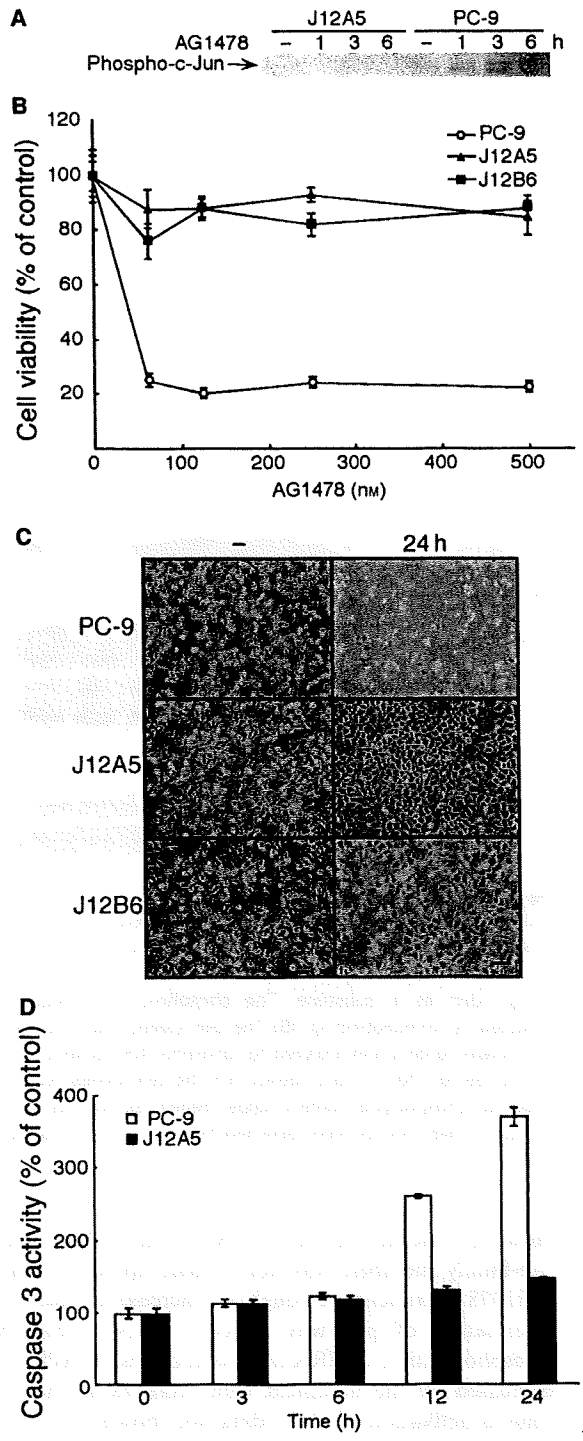

Fig. 3. Expression of dominant-negative JNK prevents AG1478-induced apoptosis. (A) Subconfluent PC-9 and J12A5 cells were incubated with 500 nM AG1478 for the indicated times. JNK activity was determined as described in Experimental Procedures. (B) PC-9, J12A5 and J12B6 cells were incubated with the indicated concentrations of AG1478 for 48 h. The viability of cells was determined by conducting WST-8 assays. The reading obtained for untreated cells was considered as 100% viability. The data presented are the mean ± SD (n = 6). (C) Phase-contrast photomicrographs were taken 24 h after incubation with 500 nM AG1478. Scale bar, 100 μm. (D) PC-9 and J12A5 cells were treated with 500 nM AG1478. Lysates were prepared at the indicated time points after the AG1478 addition and analyzed for caspase **3** activity by using a fluorometric substrate-based assay. Each point is the mean of the triplicate samples, and the bar represents the standard deviation. Similar results were obtained from three separate experiments.

inactivation of JNK should suppress this AG1478-induced apoptosis. To test this scenario, we stably transfected PC-9 cells with a mammalian expression vector encoding a dominant-negative form of JNK, and isolated two clones, J12A5 and J12B6. The results of a JNK kinase assay confirmed that J12A5 cells had no detectable activity (Fig. 3A). A colorimetric assay for cell viability, microscopic observation of cells, and an assay for caspase **3** activity revealed that this dominant-negative kinase efficiently blocked AG1478-induced apoptosis (Fig. 3B–D), indicating that activation of JNK mediated the AG1478-induced apoptosis.

A multitude of stimuli including osmotic stress activate JNK through phosphorylation of the JNK kinases MKK4 and MKK7 [18,31]. To examine the mechanism by which AG1478 induced JNK activation, we incubated PC-9 cells in the presence of AG1478 for several periods, and then prepared cell lysates from these cells to determine the phosphorylation of MKK4 and MKK7 by immunoblotting (Fig. 4A). No phosphorylated MKK4 or MKK7 was observed in the presence of AG1478, although phosphorylation of both JNK kinases in response to osmotic stress could be detected. Next, we determined the effect of AG1478 on the levels of MAPK phosphatases MKP-1 and MKP-2. As shown in Fig. 4B, AG1478 decreased the expression of the MKP-1 protein. As for the MKP-2 protein, however, AG1478 did not affect its expression level.

To check the role of MKP-1 as an anti-apoptotic signal molecule, we constitutively expressed MKP-1 in PC-9 cells. The cells were transfected with a vector directing the expression of MKP-1; and two clones, M1A4 and M1B2, were isolated as cell lines overexpressing MKP-1 (Fig. 5A). Using PC-9 and M1A4 cells, we examined the effect of AG1478 on the amounts of dually phosphorylated JNK (Fig. 5B). In PC-9 cells, AG1478 treatment decreased the expression of the MKP-1 protein and concomitantly stimulated the phosphorylation of JNK. However, the expression

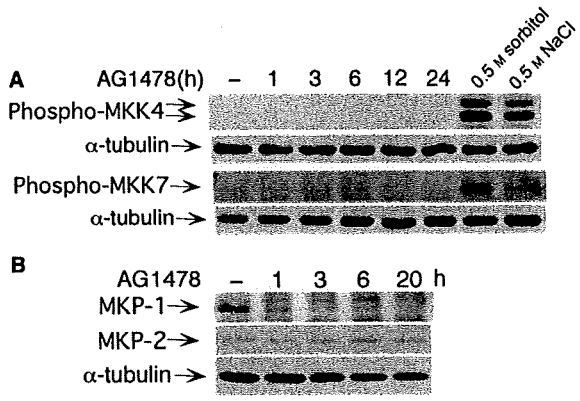

Fig. 4. Effect of AG1478 on phosphorylation of MKK4 and MKK7, and expression of MKP-1 and MKP-2. A, PC-9 cells were treated with 500 nM AG1478 for the indicated periods, and cellular lysates were analyzed by SDS/PAGE and immunoblotting with anti-[phospho SEK1/MKK4 (Ser254/Thr261)] Ig and anti-[phospho MKK7 (Ser271/Thr275)] Ig, respectively (upper). α-Tubulin levels were examined as a control for equal loading (lower). As a control for MKK4 and MKK7 activation, parallel cultures were treated with 0.5 M sorbitol for 30 min or with 0.5 M sodium chloride for 15 min. (B) The cellular lysates were prepared at the indicated time points after AG1478 treatment. Total protein (40 μg) was subjected to immunoblotting, and the membranes were hybridized with antibodies against MKP-1 (upper) or MKP-2 (middle). The equal loading of the samples was checked by using an antibody against α-tubulin (lower). The experiments corresponding to (A) and (B) were repeated three times with similar results.

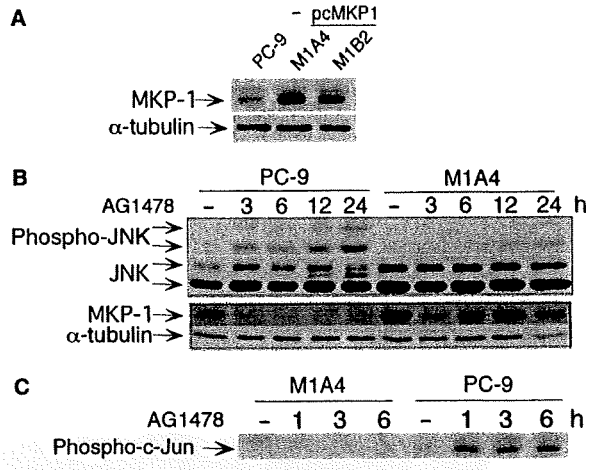

Fig. 5. Expression of MKP-1 prevents JNK activation. (A) Cellular lysates were prepared from parent PC-9 cells and pcMKP1- transfected PC-9 cells (M1A4 and M1B2). The lysates were analyzed by SDS/PAGE and immunoblotting with specific antibody against MKP-1 (upper) or α-tubulin (lower). (B) Subconfluent PC-9 and M1A4 cells were incubated with 500 nM AG1478 for the indicated times. The cells were then harvested, and equal aliquots of protein extracts (40 μg per lane) were analyzed for phospho-JNK (upper) and MKP-1 (lower) by immunoblotting. Each membrane was reprobed with JNK (upper) or an α-tubulin antibody (lower). Similar results were obtained from three separate experiments. (C) Cell lysates were prepared from PC-9 and M1A4 cells at the indicated time points after treatment with 500 nM AG1478. JNK activity was determined as described in Experimental procedures. The experiments were repeated three times with similar results.

level of MKP-1 in M1A4 cells remained high, in contrast to that in PC-9 cells; although MKP-1 expression was lowered once at 3 h after AG1478 treatment. JNK phosphorylation was extremely low in M1A4 cells. The expression patterns of MKP-1 and phospho-JNK seen in M1A4 were also observed in M1B2 cells (data not shown). The results of the JNK kinase assay indicated that JNK was not activated in M1A4 cells, where the MKP-1 expression level remained high even after exposure to AG1478 (Fig. 5C).

We next tested whether the expression level of MKP-1 correlated with sensitivity to AG1478. As shown in Fig. 6A,B, overexpression of MKP-1 resulted in resistance to AG1478. We also examined whether AG1478 could activate the effector caspase 3 in M1A4 cells (Fig. 6C). In PC-9 cells, activation of caspase 3 was observed with a maximal increase (480%) at 24 h after AG1478 treatment; however, in M1A4 cells, only a slight increase in caspase 3 enzyme activity (28% and 39% at 12 and 24 h, respectively) was detected. These results show that the MKP-1 expression level correlated with the susceptibility to AG1478-induced apoptosis.

Discussion

Gefitinib, an EGFR-tyrosine kinase inhibitor, has been reported to inhibit cell survival and proliferation signaling pathways such as MAPK and PtdIns3K/Akt pathways [10–13]. Furthermore, some reports have shown that gefitinib reduces Akt activity only in NSCLC cell lines, in which it inhibits growth [14,32]. The ErbB family of receptor tyrosine kinases includes four members, namely, the EGFR (ErbB1), ErbB2, ErbB3 and ErbB4. Among these members, ErbB3 effectively couples to the PtdIns3K/Akt pathway. Therefore, it is likely that ErbB3 serves to couple EGFR to the PtdIns3K/Akt pathway and that ErbB3 expression serves as an effective predictor of sensitivity to gefitinib in NSCLC cell lines [14]. In this study, we used PC-9 cells, which are gefitinib-sensitive human NSCLC cells with a mutation (delE746-A750) in their EGFR. In these PC-9 cells, autophosphorylation of EGFR took place independent of EGF, and it was suppressed by AG1478. Because AG1478 inhibited the phosphorylation of multiple down-stream targets including ERK1/2 in the PC-9 cells, but its effect on Akt phosphorylation was not so

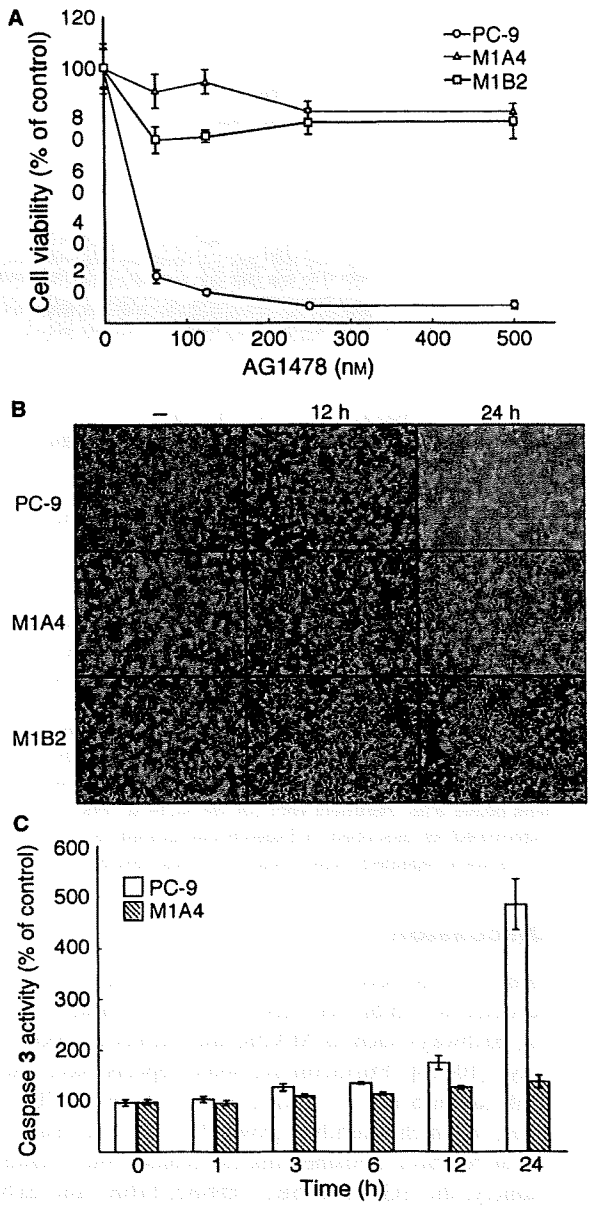

Fig. 6. Expression of MKP-1 prevents AG1478-induced apoptosis. A, PC-9, M1A4, and M1B2 cells were incubated with the indicated concentrations of AG1478 for 48 h. The viability of cells was determined by conducting WST-8 assays. The reading obtained for untreated cells was considered as 100% viability. The data presented are the mean ± SD (n = 6). (B) Phase-contrast photomicrographs were taken 12 and 24 h after incubation with 500 nM AG1478. Scale bar, 100 μm. (C) PC-9 and M1A4 cells were treated with 500 nM AG1478. Lysates were prepared at the indicated time points after the AG1478 addition and analyzed for caspase **3** activity by using a fluorometric substrate-based assay. Each point is the mean of the triplicate samples, and the bar represents the standard deviation. Similar results were obtained from three separate experiments.

significant (K. Takeuchi & F. Ito, unpublished data), intracellular signaling pathways other than PtdIns3K/Akt could be responsible for the AG1478-induced apoptosis in PC-9 cells.

Stress stimuli that induce apoptosis, including UV- and γ-irradiation, heat shock, protein synthesis inhibitors, DNA-damaging agents and the proinflammatory cytokines, are potent activators of JNK. Several anti-neoplastic agents such as cisplatin, etoposide, camptothecin and taxol, which are also strong inducers of apoptosis, also activate the JNK pathway [33]. In this study, we found that AG1478 induced the activation of JNK in PC-9 cells. Furthermore, a dominant-negative form of JNK efficiently blocked AG1478-induced apoptosis. It thus appears that EGFR-tyrosine kinase inhibitors induce apoptosis in PC-9 cells via activation of JNK.

ERK1 and ERK2, also known as p44 and p42 MAPK, respectively, represent the prototypical MAPK in mammalian cells. ERK MAP kinase catalytic activation was observed in PC-9 cells, and it was inhibited by AG1478. Increased phosphorylation of the other MAPK family member, p38, was also observed at 24 h after AG1478 treatment; but it was not observed at 12 h when apoptosis could be detected (Figs 1A and 2C). Our experiment indicated that neither SB203580 nor PD98059, inhibitors of p38 and ERK1/2, respectively, affected AG1478-induced apoptosis in PC-9 cells. Taken together, our data indicate that JNK, but not other MAPK family members such as p38 and ERK1/2, mainly transmits the apoptotic signal of AG1478 in the PC-9 cells.

JNK signaling can regulate apoptosis both positively and negatively, depending on the cell type, cellular context and the nature and dose of treatment [22,23]. Strong and sustained JNK activation is predominantly associated with induction or enhancement of apoptosis, whereas transient JNK activation can result in cell survival [23,24]. AG1478 induced strong and sustained JNK activation in PC-9 cells (Fig. 2A,B). This finding strengthens the possibility that JNK is a mediator of the apoptotic action of AG1478.

JNK activity in cells is tightly controlled by both protein kinases such as MKK4 or MKK7 and protein phosphatases such as MKPs. MKP-1, the first member of the MKP family to be identified as an ERK-specific phosphatase, is also able to inactivate JNK and p38 [34–38]. MKP-1 is an immediate-early gene whose expression is regulated by mitogenic, inflammatory and DNA-damaging stimuli [39–41]. In this study, we observed no activation of MKK4 or MKK7 in AG1478-treated PC-9 cells (Fig. 4A). However, the expression level of MKP-1, but not that of MKP-2,

was significantly decreased by the AG1478 treatment (Fig. 4B), indicating that JNK activity in the PC-9 cells may be regulated by MKP-1. Another member of the dual-phosphatase family of proteins, MKP-2 shows a 60% sequence homology to MKP-1, and also similar substrate specificity [42]. However, the expression level of MKP-2 was not affected by AG1478 treatment, indicating that the expression of MKP-1, but not that of MKP-2, is controlled by signals via EGFRs.

Brondello *et al.* reported that activation of the ERK cascade is sufficient to promote the expression of MKP-1 and MKP-2 [43]. It has also been suggested that MKP-1 expression is regulated by ERK-dependent and -independent signals [44]. Because the ERK inhibitor PD98059 did not affect MKP-1 expression or activation of JNK in PC-9 cells (K. Takeuchi & F. Ito, unpublished data), MPK-1 expression in PC-9 cells may be controlled in an ERK-independent manner. Recently, Ryser *et al.* reported that MKP-1 transcription is regulated in the transcriptional elongation step: under basal conditions, a strong block to elongation in the first exon regulates MKP-1 gene transcription [45]. Thus, EGFR-mediated signals may overcome this block to stimulate MKP-1 gene transcription in PC-9 cells. Another possible mechanism responsible for EGFR-mediated enhancement of MKP-1 expression is that MKP-1 degradation via the ubiquitin–proteasome pathway is suppressed by EGFR activation. In fact, some research groups have reported that the expression level of MKP-1 is controlled via the ubiquitin–proteasome pathway [46,47]. Our preliminary experiment also indicated that AG1478-induced MKP-1 degradation was suppressed in the presence of proteasome inhibitors such as MG-132 and ALLN (K. Takeuchi & F. Ito, unpublished data).

Gene disruption studies demonstrate that JNK is required for the release of mitochondrial proapoptotic molecules (including cytochrome *c*) and apoptosis in response to UV radiation [48]. Bax and Bak (members of the proapoptotic group of multidomain Bcl-2-related proteins) are essential for the JNK-stimulated release of cytochrome *c* and apoptosis [49]. Other studies have shown that 14-3-3 proteins are direct targets of JNK and that phosphorylation of 14-3-3 proteins by JNK results in dissociation of Bax from 14-3-3 proteins, leading to apoptosis [50]. Because translocation of Bax to mitochondria was observed in AG1478-treated PC-9 cells (K. Takeuchi & F. Ito, unpublished data), AG1478 may exert its apoptotic actions, at least in part, by promoting the translocation of Bax to mitochondria.

Some reports have shown that the activation of the Fas/FasL system may be one of the mechanisms responsible for drug-induced apoptosis in a variety of cancer cells of different histotype [51]. Chang *et al.* recently reported that an increase in Fas protein expression might be the molecular mechanism by which gefitinib induces apoptosis in lung cancer cell lines [52]. Furthermore, it has been reported that c-Jun-dependent FasL expression plays a critical role in the induction of apoptosis by genotoxic agents [53]. To understand the causal relationship between JNK activation and AG1478-induced apoptosis, we need to study whether AG1478 induces the expression of Fas or FasL in PC-9 cells.

Overexpression of MKP-1 inhibited the AG1478-induced JNK activation and also AG1478-induced apoptosis. These results indicate that there is a link between the decreased MKP-1 activity and AG1478-induced apoptosis: MKP-1 expression is controlled by signals downstream of EGFR, and it is downregulated in the presence of an inhibitor of EGFR tyrosine kinase. This downregulation could be followed by JNK activation, triggering the apoptosis pathway.

Understanding the molecular basis of responsiveness to gefitinib is important to identify patients who will have a positive response to this drug. The EGFR gene in tumors from patients with gefitinib-responsive lung cancer was recently examined for mutations, and clustering of mutations was detected in the part of the gene encoding the ATP-binding pocket. Screening for such mutations may identify patients who will have a positive response to the drug. However, this study showed that NSCLC cell line PC-9 was dependent on the MKP-1/JNK pathway for its growth and survival. Thus, sensitivity to gefitinib may be predicted from the detailed analysis of the MKP-1/JNK pathway as described in this study. Although the MKP-1 level in normal cells is low, an increased level of MKP-1 has been found in human ovarian, breast, and prostate cancer [54–56]. Our results suggest that MKP-1 may be a candidate drug target in order to optimize gefitinib-based therapeutic protocols.

Experimental procedures

Materials

EGF (ultra-pure) from mouse submaxillary glands was purchased from Toyobo Co., Ltd (Osaka, Japan). Fetal calf serum came from Gibco (Grand Island, NY, USA). Phenylmethanesulfonyl fluoride, pepstatin A, aprotinin and leupeptin were obtained from Sigma (St Louis, MO, USA). RPMI-1640 medium was from Nissui Pharmaceutical Co., Ltd (Tokyo, Japan). Antibodies used and their sources were: ERK1/2 (pT202/pY204) phospho-specific antibody (clone 20A), JNK(pT183/pY185) phospho-specific antibody

(clone 41), p38 MAPK (pT180/pY182) phospho-specific antibody (clone 36), p38α antibody (clone 27), MKP2 antibody (clone 48) and pan-JNK/SAPK1 antibody (clone 37), from BD Transduction Laboratories (San Jose, CA, USA); MKP-1 antibody (C-19), from Santa Cruz Biotechnology (Santa Cruz, CA, USA); α-tubulin antibody (clone B-5-1-2) and MAP kinase antibody, from Sigma; phospho-SEK1/MKK4 (Ser254/Thr261) antibody and phospho-MKK7 (Ser271/Thr275) antibody, from Cell Signaling Technology (Danvers, MA, USA); swine horseradish peroxidase (HRP)-linked anti-rabbit Ig, from DAKO (Glostrup, Denmark); and sheep HRP-linked anti-mouse Ig, from GE Healthcare UK Ltd (Amersham, UK). Plasmid pcMKP1 was generated from *Homo sapiens* dual-specificity phosphatase 1 cDNA, MGC clone (ID 4794895) purchased from Invitrogen (Carlsbad, CA, USA). The MGC clone had been cloned into pBluscriptR. This clone was digested with *Ava*I, treated with T4 DNA polymerase, ligated to the pcDNA 3.1 mammalian expression vector (Invitrogen) prepared by digestion with *Eco*RV and treated with calf intestinal phosphatase to produce pcMKP1. Plasmid DNA was prepared by standard techniques (Qiagen Plasmid Midi Kit). pBabePuro, a puromycin-resistant vector, was kindly provided by K. Shuai (UCLA, USA). pcDL-SRα296JNK2(VPF), a dominant-negative JNK expression vector, was kindly donated by E. Nishida (Kyoto University, Japan).

Cell culture and transfection

Human non-small cell lung cancer cell line PC-9 was cultured to subconfluence in RPMI-1640 medium supplemented with 5% fetal calf serum and used for all of the experiments. PC-9 cells were plated 24 h before transfection and co-transfected with 8.5 μg of pcDL-SRα 296JNK2(VPF) or pcMKP-1 and 1.5 μg of pBabePuro by using the Lipofectamine reagent, and the transfected cells were selected by exposure to 2.5 mg of puromycin (Sigma) per mL of medium for 3 weeks. Empty vector and pBabePuro were used for co-transfection as a negative control. The expression of JNK protein and MKP-1 protein were verified by immunoblot analysis using anti-(pan-JNK/SAPK1 aa264–415) and anti-(MKP-1) (Santa Cruz Biotechnology), respectively.

Determination of cell viability

The anti-proliferative effect of AG1478 on PC-9 cells was assessed by using a Cell Counting Kit-8 (DOJIN, Kumamoto, Japan) according to the manufacturer's instructions. The Cell Counting Kit-8 is a colorimetric method in which the intensity of the dye is proportional to the number of the viable cells. Briefly, 200 μL of a suspension of PC-9 cells was seeded into each well of a 96-well plate at a density of 2000 cells·well^{-1}. After 48 h, the culture medium was replaced with 100 μL of AG1478 solution at various concentrations. After incubation for 48 h at 37 °C, 10 μL of WST-8 solution was added to each well, and the cells were incubated for a further 40 min at 37 °C. A_{450} was measured using a Bio-Rad microplate reader model 550. Each experiment was performed by using six replicate wells for each drug concentration and was carried out independently three times.

Preparation of cellular lysates and immunoblotting

Preparation of cellular lysates and immunoblotting were performed as described previously [57]. Briefly, cells were lysed with buffer A (20 mM Tris/HCl, pH 7.4, containing 137 mM NaCl, 2 mM EGTA, 5 mM EDTA, 1% Nonidet P-40, 1% Triton X-100, 100 μg·mL^{-1} phenylmethanesulfonyl fluoride, 1 μg·mL^{-1} pepstatin A, 1 μg·mL^{-1} *p*-toluenesulfonyl-L-arginine methyl ester, 2 μg·mL^{-1} leupeptin, 1 mM sodium orthovanadate, 50 mM sodium fluoride and 30 mM $Na_4P_2O_7$). Lysates were then incubated on ice for 30 min, and the insoluble material was cleared by centrifugation. Samples were normalized for protein content and separated by SDS/PAGE, after which they were transferred to an Immobilon-P membrane (Millipore, Bedford, MA, USA) for immunoblotting with antibodies.

Caspase 3 activity assay

Caspase activity was assayed as described previously [57]. Briefly, cells were lysed with buffer A, and the protein concentration in each sample was adjusted to 100 μg·50 μL^{-1} of buffer A. Fifty microliters of 2× Reaction Buffer (0.2 M Hepes/NaOH, pH 7.4, containing 20% sucrose, 0.2% Chaps and 1 mM dithiothreitol) was added to each sample, which was then incubated with Z-DEVD-AFC substrate (50 μM final concentration) at 37 °C for 1 h. The samples were read in a fluorometer (VersaFluor; Bio-Rad) equipped with a 340–380 nm excitation filter (EX 360/40) and 505–515 nm emission filter (EM 510/10).

JNK assay

PC-9 cells were cultured in RPMI-1640 supplemented with 5% fetal calf serum at a density of 6.0×10^5 per 100 mm dish for 2 days and then assayed for JNK activity. JNK assays were performed by using a SAPK/JNK Assay kit (Cell Signaling Technology) according to the manufacturer's specifications. In brief, after various times of treatment with AG1478, adherent cells and floating cells were harvested by centrifugation and washed once in NaCl/P_i. Subsequently, the cells were lysed with lysis buffer (consisting of 20 mM Tris/HCl, pH 7.4, containing 150 mM NaCl, 1 mM EDTA, 1 mM EGTA, 1% Triton X-100, 2.5 mM $Na_4P_2O_7$, 1 mM β-glycerophosphate, 1 mM Na_3VO_4, 1 nM

deltamethrin, 180 nM nodularin, 100 $\mu g \cdot mL^{-1}$ phenylmethanesulfonyl fluoride, 25 $\mu g \cdot mL^{-1}$ aprotinin, 25 $\mu g \cdot mL^{-1}$ leupeptin and 25 $\mu g \cdot mL^{-1}$ pepstatin), and scraped into microcentrifuge tubes. Extracts were prepared by sonicating each sample on ice (BRANSON SONIFIER 250, Danbury, CT, USA), and insoluble material was removed by microcentrifugation. Soluble fractions were mixed with 2 μg glutathione *S*-transferase–c-Jun (1–89) agarose beads (Cell Signaling Technology) and rotated overnight at 4 °C. JNK–c-Jun complexes were collected and washed with lysis buffer followed by kinase buffer, consisting of 25 mM Tris/HCl, pH 7.5, 5 mM β-glycerophosphate, 2 mM Cleland's reagent, 0.1 mM Na_3VO_4 and 10 mM $MgCl_2$. The *in vitro* kinase reaction was initiated by the addition of kinase buffer containing 100 μM ATP, samples were incubated at 30 °C for 45 min, and reactions were terminated by the addition of SDS sample buffer and heating to 95 °C for 5 min. Phosphorylated c-Jun was detected by western blotting using a phospho-specific c-Jun antibody (Cell Signaling Technology).

Hoechst- PI staining

For the study of nuclear morphologic changes induced by AG1478, PC-9 cells were seeded on coverslips, grown to sub-confluence, and treated with AG1478 for the desired times. After fixation with formalin solution, the cells were stained with 10 μM Hoechst33342 and 10 μM PI in 5% fetal calf serum/RPMI. Coverslips were mounted on slides by using Dakocytomation Fluorescent Mounting Medium (DAKO) and observed under a fluorescence microscope (Axioskop; Carl Zeiss, Jena, Germany).

Acknowledgements

We thank Dr K. Shuai for providing the pbabePuro, Dr E. Nishida for pcDL-SRα296JNK2(VPF), a dominant-negative JNK expression vector, and Y. Inoue, Y. Kaji and Y. Hasegawa for technical assistance. This work was supported in part by a grant-in-aid for scientific research from the Ministry of Education, Culture, Sports, Science, and Technology of Japan, and by funding from the Fugaku Trust for Medical Research.

References

1 Burgess AW, Cho HS, Eigenbrot C, Ferguson KM, Garrett TP, Leahy DJ, Lemmon MA, Sliwkowski MX, Ward CW & Yokoyama S (2003) An open-and-shut case? Recent insights into the activation of EGF/ErbB receptors. *Mol Cell* **12**, 541–552.

2 Citri A & Yarden Y (2006) EGF–ERBB signalling: towards the systems level. *Nat Rev Mol Cell Biol* **7**, 505–516.

3 Herbst RS & Bunn PA Jr (2003) Targeting the epidermal growth factor receptor in non-small cell lung cancer. *Clin Cancer Res* **9**, 5813–5824.

4 Nakagawa K, Tamura T, Negoro S, Kudoh S, Yamamoto N, Yamamoto N, Takeda K, Swaisland H, Nakatani I, Hirose M *et al.* (2003) Phase I pharmacokinetic trial of the selective oral epidermal growth factor receptor tyrosine kinase inhibitor gefitinib ('Iressa', ZD1839) in Japanese patients with solid malignant tumors. *Ann Oncol* **14**, 922–930.

5 Gazdar AF, Shigematsu H, Herz J & Minna JD (2004) Mutations and addiction to EGFR: the Achilles 'heal' of lung cancers? *Trends Mol Med* **10**, 481–486.

6 Lynch TJ, Bell DW, Sordella R, Gurubhagavatula S, Okimoto RA, Brannigan BW, Harris PL, Haserlat SM, Supko JG, Haluska FG *et al.* (2004) Activating mutations in the epidermal growth factor receptor underlying responsiveness of non-small-cell lung cancer to gefitinib. *N Engl J Med* **350**, 2129–2139.

7 Paez JG, Jänne PA, Lee JC, Tracy S, Greulich H, Gabriel S, Herman P, Kaye FJ, Lindeman N, Boggon TJ *et al.* (2004) EGFR mutations in lung cancer: correlation with clinical response to gefitinib therapy. *Science* **304**, 1497–1500.

8 Pao W, Miller V, Zakowski M, Doherty J, Politi K, Sarkaria I, Singh B, Heelan R, Rusch V, Fulton L *et al.* (2004) EGF receptor gene mutations are common in lung cancers from 'never smokers' and are associated with sensitivity of tumors to gefitinib and erlotinib. *Proc Natl Acad Sci USA* **101**, 13306–13311.

9 Gilmore AP, Valentijn AJ, Wang P, Ranger AM, Bundred N, O'Hare MJ, Wakeling A, Korsmeyer SJ & Streuli CH (2002) Activation of BAD by therapeutic inhibition of epidermal growth factor receptor and transactivation by insulin-like growth factor receptor. *J Biol Chem* **277**, 27643–27650.

10 Janmaat ML, Kruyt FA, Rodriguez JA & Giaccone G (2003) Response to epidermal growth factor receptor inhibitors in non-small cell lung cancer cells: limited antiproliferative effects and absence of apoptosis associated with persistent activity of extracellular signal-regulated kinase or Akt kinase pathways. *Clin Cancer Res* **9**, 2316–2326.

11 Anderson NG, Ahmad T, Chan K, Dobson R & Bundred NJ (2001) ZD1839 (Iressa), a novel epidermal growth factor receptor (EGFR) tyrosine kinase inhibitor, potently inhibits the growth of EGFR-positive cancer cell lines with or without erbB2 overexpression. *Int J Cancer* **94**, 774–782.

12 Moasser MM, Basso A, Averbuch SD & Rosen N (2001) The tyrosine kinase inhibitor ZD1839 ('Iressa') inhibits HER2-driven signaling and suppresses the growth of HER2-overexpressing tumor cells. *Cancer Res* **61**, 7184–7188.

13 Moulder SL, Yakes FM, Muthuswamy SK, Bianco R, Simpson JF & Arteaga CL (2001) Epidermal growth factor receptor (HER1) tyrosine kinase inhibitor ZD1839 (Iressa) inhibits HER2/neu (erbB2)-over-expressing breast cancer cells *in vitro* and *in vivo*. *Cancer Res* **61**, 8887–8895.
14 Engelman JA, Jänne PA, Mermel C, Pearlberg J, Mukohara T, Fleet C, Cichowski K, Johnson BE & Cantley LC (2005) ErbB-3 mediates phosphoinositide 3-kinase activity in gefitinib-sensitive non-small cell lung cancer cell lines. *Proc Natl Acad Sci USA* **102**, 3788–3793.
15 Ariyama H, Qin B, Baba E, Tanaka R, Mitsugi K, Harada M & Nakano S (2006) Gefitinib, a selective EGFR tyrosine kinase inhibitor, induces apoptosis through activation of Bax in human gallbladder adenocarcinoma cells. *J Cell Biochem* **97**, 724–734.
16 Miyata Y & Nishida E (1999) Distantly related cousins of MAP kinase: biochemical properties and possible physiological functions. *Biochem Biophys Res Commun* **266**, 291–295.
17 Johnson GL & Lapadat R (2002) Mitogen-activated protein kinase pathways mediated by ERK, JNK, and p38 protein kinases. *Science* **298**, 1911–1912.
18 Morrison DK & Davis RJ (2003) Regulation of MAP kinase signaling modules by scaffold proteins in mammals. *Annu Rev Cell Dev Biol* **19**, 91–118.
19 Hibi M, Lin A, Smeal T, Minden A & Karin M (1993) Identification of an oncoprotein- and UV-responsive protein kinase that binds and potentiates the c-Jun activation domain. *Genes Dev* **7**, 2135–2148.
20 Kyriakis JM, Banerjee P, Nikolakaki E, Dai T, Rubie EA, Ahmad MF, Avruch J & Woodgett JR (1994) The stress-activated protein kinase subfamily of c-Jun kinases. *Nature* **369**, 156–160.
21 Kharbanda S, Ren R, Pandey P, Shafman TD, Feller SM, Weichselbaum RR & Kufe DW (1995) Activation of the c-Abl tyrosine kinase in the stress response to DNA-damaging agents. *Nature* **376**, 785–788.
22 Davis RJ (2000) Signal transduction by the JNK group of MAP kinases. *Cell* **103**, 239–252.
23 Chang NS (2001) Hyaluronidase activation of c-Jun N-terminal kinase is necessary for protection of L929 fibrosarcoma cells from staurosporine-mediated cell death. *Biochem Biophys Res Commun* **283**, 278–286.
24 Lamb JA, Ventura JJ, Hess P, Flavell RA & Davis RJ (2003) JunD mediates survival signaling by the JNK signal transduction pathway. *Mol Cell* **11**, 1479–1489.
25 Wada T, Joza N, Cheng HY, Sasaki T, Kozieradzki I, Bachmaier K, Katada T, Schreiber M, Wagner EF, Nishina H *et al.* (2004) MKK7 couples stress signalling to G2/M cell-cycle progression and cellular senescence. *Nat Cell Biol* **6**, 215–226.
26 Camps M, Nichols A & Arkinstall S (2000) Dual specificity phosphatases: a gene family for control of MAP kinase function. *FASEB J* **14**, 6–16.
27 Keyse SM (2000) Protein phosphatases and the regulation of mitogen-activated protein kinase signalling. *Curr Opin Cell Biol* **12**, 186–192.
28 Farooq A & Zhou MM (2004) Structure and regulation of MAPK phosphatases. *Cell Signal* **16**, 769–779.
29 Chen YR, Wang X, Templeton D, Davis RJ & Tan TH (1996) The role of c-Jun N-terminal kinase (JNK) in apoptosis induced by ultraviolet C and gamma radiation. Duration of JNK activation may determine cell death and proliferation. *J Biol Chem* **271**, 31929–31936.
30 Verheij M, Bose R, Lin XH, Yao B, Jarvis WD, Grant S, Birrer MJ, Szabo E, Zon LI, Kyriakis JM *et al.* (1996) Requirement for ceramide-initiated SAPK/JNK signalling in stress-induced apoptosis. *Nature* **380**, 75–79.
31 Sánchez-Pérez I, Martínez-Gomariz M, Williams D, Keyse SM & Perona R (2000) CL100/MKP-1 modulates JNK activation and apoptosis in response to cisplatin. *Oncogene* **19**, 5142–5152.
32 Sordella R, Bell DW, Haber DA & Settleman J (2004) Gefitinib-sensitizing EGFR mutations in lung cancer activate anti-apoptotic pathways. *Science* **305**, 1163–1167.
33 Seimiya H, Mashima T, Toho M & Tsuruo T (1997) c-Jun N-terminal kinase-mediated activation of interleukin-1beta converting enzyme/CED-3-like protease during anticancer drug-induced apoptosis. *J Biol Chem* **272**, 4631–4636.
34 Chu Y, Solski PA, Khosravi-Far R, Der CJ & Kelly K (1996) The mitogen-activated protein kinase phosphatases PAC1, MKP-1, and MKP-2 have unique substrate specificities and reduced activity in vivo toward the ERK2 sevenmaker mutation. *J Biol Chem* **271**, 6497–6501.
35 Franklin CC & Kraft AS (1995) Constitutively active MAP kinase kinase (MEK1) stimulates SAP kinase and c-Jun transcriptional activity in U937 human leukemic cells. *Oncogene* **11**, 2365–2374.
36 Gupta S, Barrett T, Whitmarsh AJ, Cavanagh J, Sluss HK, Dérijard B & Davis RJ (1996) Selective interaction of JNK protein kinase isoforms with transcription factors. *EMBO J* **15**, 2760–2770.
37 Liu Y, Gorospe M, Yang C & Holbrook NJ (1995) Role of mitogen-activated protein kinase phosphatase during the cellular response to genotoxic stress. Inhibition of c-Jun N-terminal kinase activity and AP-1-dependent gene activation. *J Biol Chem* **270**, 8377–8380.
38 Raingeaud J, Gupta S, Rogers JS, Dickens M, Han J, Ulevitch RJ & Davis RJ (1995) Pro-inflammatory cytokines and environmental stress cause p38 mitogen-activated protein kinase activation by dual phosphorylation on tyrosine and threonine. *J Biol Chem* **270**, 7420–7426.

39 Beltman J, McCormick F & Cook SJ (1996) The selective protein kinase C inhibitor, Ro-31-8220, inhibits mitogen-activated protein kinase phosphatase-1 (MKP-1) expression, induces c-Jun expression, and activates Jun N-terminal kinase. *J Biol Chem* **271**, 27018–27024.

40 Sánchez-Perez I, Murguía JR & Perona R (1998) Cisplatin induces a persistent activation of JNK that is related to cell death. *Oncogene* **16**, 533–540.

41 Li J, Gorospe M, Hutter D, Barnes J, Keyse SM & Liu Y (2001) Transcriptional induction of MKP-1 in response to stress is associated with histone H3 phosphorylation-acetylation. *Mol Cell Biol* **21**, 8213–8224.

42 Hirsch DD & Stork PJ (1997) Mitogen-activated protein kinase phosphatases inactivate stress-activated protein kinase pathways *in vivo*. *J Biol Chem* **272**, 4568–4575.

43 Brondello JM, Brunet A, Pouysségur J & McKenzie FR (1997) The dual specificity mitogen-activated protein kinase phosphatase-1 and -2 are induced by the p42/p44MAPK cascade. *J Biol Chem* **272**, 1368–1376.

44 Cook SJ, Beltman J, Cadwallader KA, McMahon M & McCormick F (1997) Regulation of mitogen-activated protein kinase phosphatase-1 expression by extracellular signal-related kinase-dependent and Ca^{2+}-dependent signal pathways in Rat-1 cells. *J Biol Chem* **272**, 13309–13319.

45 Ryser S, Tortola S, van Haasteren G, Muda M, Li S & Schlegel W (2001) MAP kinase phosphatase-1 gene transcription in rat neuroendocrine cells is modulated by a calcium-sensitive block to elongation in the first exon. *J Biol Chem* **276**, 33319–33327.

46 Lin YW, Chuang SM & Yang JL (2003) ERK1/2 achieves sustained activation by stimulating MAPK phosphatase-1 degradation via the ubiquitin-proteasome pathway. *J Biol Chem* **278**, 21534–21541.

47 Brondello JM, Pouysségur J & McKenzie FR (1999) Reduced MAP kinase phosphatase-1 degradation after p42/p44MAPK-dependent phosphorylation. *Science* **286**, 2514–2517.

48 Tournier C, Hess P, Yang DD, Xu J, Turner TK, Nimnual A, Bar-Sagi D, Jones SN, Flavell RA & Davis RJ (2000) Requirement of JNK for stress-induced activation of the cytochrome *c*-mediated death pathway. *Science* **288**, 870–874.

49 Lei K, Nimnual A, Zong WX, Kennedy NJ, Flavell RA, Thompson CB, Bar-Sagi D & Davis RJ (2002) The Bax subfamily of Bcl2-related proteins is essential for apoptotic signal transduction by c-Jun NH(2)-terminal kinase. *Mol Cell Biol* **22**, 4929–4942.

50 Tsuruta F, Sunayama J, Mori Y, Hattori S, Shimizu S, Tsujimoto Y, Yoshioka K, Masuyama N & Gotoh Y (2004) JNK promotes Bax translocation to mitochondria through phosphorylation of 14-3-3 proteins. *EMBO J* **23**, 1889–1899.

51 Scaffidi C, Fulda S, Srinivasan A, Friesen C, Li F, Tomaselli KJ, Debatin KM, Krammer PH & Peter ME (1998) Two CD95 (APO-1/Fas) signaling pathways. *EMBO J* **17**, 1675–1687.

52 Chang GC, Hsu SL, Tsai JR, Liang FP, Lin SY, Sheu GT & Chen CY (2004) Molecular mechanisms of ZD1839-induced G1-cell cycle arrest and apoptosis in human lung adenocarcinoma A549 cells. *Biochem Pharmacol* **68**, 1453–1464.

53 Kolbus A, Herr I, Schreiber M, Debatin KM, Wagner EF & Angel P (2000) c-Jun-dependent CD95-L expression is a rate-limiting step in the induction of apoptosis by alkylating agents. *Mol Cell Biol* **20**, 575–582.

54 Srikanth S, Franklin CC, Duke RC & Kraft RS (1999) Human DU145 prostate cancer cells overexpressing mitogen-activated protein kinase phosphatase-1 are resistant to Fas ligand-induced mitochondrial perturbations and cellular apoptosis. *Mol Cell Biochem* **199**, 169–178.

55 Denkert C, Schmitt WD, Berger S, Reles A, Pest S, Siegert A, Lichtenegger W, Dietel M & Hauptmann S (2002) Expression of mitogen-activated protein kinase phosphatase-1 (MKP-1) in primary human ovarian carcinoma. *Int J Cancer* **102**, 507–513.

56 Wang HY, Cheng Z & Malbon CC (2003) Overexpression of mitogen-activated protein kinase phosphatases MKP1, MKP2 in human breast cancer. *Cancer Lett* **191**, 229–237.

57 Takeuchi K, Motoda Y & Ito F (2006) Role of transcription factor activator protein 1 (AP1) in epidermal growth factor-mediated protection against apoptosis induced by a DNA-damaging agent. *FEBS J* **273**, 3743–3755.

nature medicine

RPN2 gene confers docetaxel resistance in breast cancer

Kimi Honma[1,2], Kyoko Iwao-Koizumi[3], Fumitaka Takeshita[1], Yusuke Yamamoto[1], Teruhiko Yoshida[4], Kazuto Nishio[5], Shunji Nagahara[6], Kikuya Kato[3] & Takahiro Ochiya[1]

Drug resistance acquired by cancer cells has led to treatment failure. To understand the regulatory network underlying docetaxel resistance in breast cancer cells and to identify molecular targets for therapy, we tested small interfering RNAs (siRNAs) against 36 genes whose expression was elevated in human nonresponders to docetaxel for the ability to promote apoptosis of docetaxel-resistant human breast cancer cells (MCF7-ADR cells). The results indicate that the downregulation of the gene encoding ribophorin II (RPN2), which is part of an *N*-oligosaccharyl transferase complex, most efficiently induces apoptosis of MCF7-ADR cells in the presence of docetaxel. RPN2 silencing induced reduced glycosylation of the P-glycoprotein, as well as decreased membrane localization, thereby sensitizing MCF7-ADR cells to docetaxel. Moreover, *in vivo* delivery of siRNA specific for *RPN2* markedly reduced tumor growth in two types of models for drug resistance. Thus, RPN2 silencing makes cancer cells hypersensitive response to docetaxel, and RPN2 might be a new target for RNA interference–based therapeutics against drug resistance.

Breast cancer is the most common malignancy in women. Either neoadjuvant or adjuvant chemotherapy administered to subjects with stage 1–3 breast cancers can improve their survival rates[1–3]. Among chemotherapeutic agents, docetaxel, which belongs to the group of taxanes (mitotic inhibitors and antimicrotubule agents), has been shown to have well-established benefits in breast cancer[4]. The response rate to docetaxel, however, is 50% even in first-line chemotherapy, and it decreases to 20–30% in second- or third-line chemotherapy[5–7]; nearly half of the treated subjects do not respond to it and suffer side effects. There is currently no method to reliably predict tumor responses to docetaxel before therapy or to detect when resistance or hypersensitivity develops. Therefore, the identification of molecular biomarkers in docetaxel-resistant breast cancer that could help in a more accurate assessment of individual treatment and the development of molecular-target therapies that could lead to better tumor reduction are of considerable interest.

It has been reported that the expression of the multidrug transporter P-glycoprotein, encoded by the *MDR1* gene (official gene symbol *ABCB1*), is one of the causes of clinical drug resistance to taxanes[8,9]. Other molecules, such as the multidrug resistance–associated protein MRP1[10,11], breast cancer resistance protein (*ABCG2*) and other transporters[12], which act as energy-dependent efflux pumps capable of expelling a large range of xenobiotics, and GSTpi, which is one of the isoenzymes of the glutathione-*S*-transferase (GST)[13–15], have been extensively reported to be overexpressed in tumor cells showing the multidrug-resistant phenotype. It was recently shown that high thioredoxin expression is associated with resistance to docetaxel in breast cancer[16,17]. These molecules might be clinically useful in the prediction of a response to anticancer drugs. Currently, however, none have proven to be specific target molecules for increasing the efficacy of chemotherapy in breast cancer.

To better understand the regulatory network underlying docetaxel resistance in breast cancer cells and to identify molecular targets for therapy, we initiated gene expression profiling of 44 subjects with breast tumors (22 responders and 22 nonresponders) by adaptor-tagged competitive PCR[18] to identify the genes capable of predicting a docetaxel response in human breast cancer and reported the preliminary results of 85 genes whose expression potentially correlated with docetaxel resistance[16]. In the current study, we used an atelocollagen-based siRNA cell transfection array[19,20] to identify the genes responsible for conferring drug resistance. Among the siRNAs targeting genes that were elevated in nonresponders to docetaxel, siRNA designed for *RPN2* (RNP2 siRNA) significantly promoted docetaxel-dependent apoptosis and cell growth inhibition of MCF7-ADR human breast cancer cells that are resistant to docetaxel. Furthermore, atelocollagen-mediated *in vivo* delivery of RPN2 siRNA significantly reduced drug-resistant tumor growth in mice given docetaxel. RPN2 confers drug resistance via the glycosylation of P-glycoproteins and regulates antiapoptotic genes. Thus, RPN2 siRNA introduction hypersensitizes cancer cell response to chemotherapeutic agents, making RPN2 a potential key target for future RNA interference (RNAi)-based therapeutics against a drug-resistant tumor.

[1]Section for Studies on Metastasis, Japanese National Cancer Center Research Institute, 1-1, Tsukiji, 5-chome, Chuo-ku, Tokyo 104-0045, Japan. [2]Koken Bioscience Institute, KOKEN, 2-13-10 Ukima, Kita-ku, Tokyo 115-0051, Japan. [3]Research Institute, Osaka Medical Center for Cancer and Cardiovascular Diseases, 1-3-2 Nakamichi, Higashinari-ku, Osaka 537-8511, Japan. [4]Genetics Division and [5]Pharmaceutical Division, Japanese National Cancer Center Research Institute, 1-1, Tsukiji, 5-chome, Chuo-ku, Tokyo 104-0045, Japan. [6]Dainippon Sumitomo Pharma, 3-45, Kurakakiuchi, 1-chome, Ibaraki, Osaka 567-0878, Japan. Correspondence should be addressed to T.O. (tochiya@ncc.go.jp).

Received 2 March; accepted 10 July; published online 17 August 2008; doi:10.1038/nm.1858

RESULTS

RNAi-based screening for identification of molecular target

As an extension of our previous strategy of analyzing docetaxel resistance in breast cancer cells and of identifying molecular targets for therapy[16], we conducted a study of RNAi-induced gene knockdown in docetaxel-resistant MCF7-ADR human breast cancer cells. Among the 85 genes listed[16], 61 genes that are potentially targets for siRNA strategy were upregulated in human nonresponders. We selected 36 genes with more than a 0.365 signal-to-noise ratio and successfully designed and synthesized siRNAs specific to these genes (**Table 1**). The siRNAs were conjugated to atelocollagen and arrayed on a 96-well microplate. Then, MCF7-ADR cells expressing the luciferase gene (MCF7-ADR-Luc) were seeded into the microplate (the target validation process by cell transfection array is schematically shown in **Supplementary Fig. 1** online.). To evaluate the efficiency of the atelocollagen-mediated cell transfection array, we used GL3 siRNA against the gene encoding luciferase. Atelocollagen-mediated GL3 siRNA delivery caused an approximate 75% reduction of the luciferase activity in MCF7-ADR-Luc cells relative to the control nontargeting siRNA (data not shown). To identify the genes responsible for docetaxel resistance, we assessed siRNAs for their ability to inhibit cell growth and induce apoptosis in the presence of docetaxel compared with the control nontargeting siRNA. We measured cell growth by luciferase activity and examined apoptosis by caspase-7 activation. The results indicated that the downregulation of eight genes (*PTPLB, GSTP1, TUBB, RPN2, SQRDL, NDUFS3, PDCD5* and *MRPL17*) resulted in marked inhibition of cell growth ($P < 0.05$, **Fig. 1a**). Induction of apoptosis was evidenced in cells by downregulation of six genes (*PTPLB, APRT, CFL1, RPN2, SQRDL* and *MRPL17*; $P < 0.05$, **Fig. 1b**). In particular, RPN2 siRNA strongly enhanced caspase-7 activity in the presence of docetaxel ($P < 0.001$, **Supplementary Fig. 2a** online). We validated these results by counting Hoechst-stained cells showing apoptotic nuclear condensation and fragmentation (**Fig. 2a**) and found that there was a significantly higher apoptotic cell death rate in cells given RPN2 siRNA and docetaxel relative to that in cells given RPN2 siRNA alone ($P < 0.02$, **Fig. 2b**). No significant difference was observed in cells with nontargeting control siRNA (**Fig. 2b**). At 72 h after treatment with siRNA and docetaxel, there was substantial cell death induced by RPN2 siRNA compared with the control nontargeting siRNA (**Fig. 2c**). At 96 h after the transfection, almost all RPN2 siRNA–treated cells were detached and disappeared from the culture dishes.

Table 1 The list of 36 genes whose expression is elevated in nonresponders to docetaxel in subjects with breast cancer

No	Gene	Description	Accession number
1	*UFM1*	Ubiquitin-fold modifier 1	BC005193
2	*PTPLB*	Protein tyrosine phosphatase-like (proline instead of catalytic arginine), member b	AF052159
3	*S100A10*	S100 calcium binding protein A10	M38591
4	*APRT*	Adenine phosphoribosyltransferase	Y00486
5	*CFL1*	Cofilin-1 (non-muscle)	X95404
6	*GSTP1*	Glutathione *S*-transferase pi 1	M24485
7	*HSPA5*	Heat shock 70 kDa protein 5 (glucose-regulated protein, 78 kDa)	M19645
8	*GNB2L1*	Guanine nucleotide binding protein (G protein), β polypeptide 2 like 1	M24194
9	*TUBB*	Tubulin, β	BC001002
10	*MX1*	Myxovirus (influenza virus) resistance 1, interferon-inducible protein p78 (mouse)	M33882
11	*COX7C*	Cytochrome *c* oxidase subunit VIIc	BC001005
12	*RPN2*	Ribophorin II	Y00282
13	*DYNLL1*	Dynein, light chain, LC8-type 1	U32944
14	*FXR1*	Fragile X mental retardation, autosomal homolog 1	U25165
15	*SQRDL*	Sulfide quinone reductase-like (yeast)	AF151802
16	*NDUFS3*	NADH dehydrogenase (ubiquinone) Fe-S protein 3, 30 kDa (NADH-coenzyme Q reductase)	AL135819
17	*EST*	ESTs	AL358933
18	*C19orf10*	Chromosome 19 open reading frame 10	BC003639
19	*ATP5E*	ATP synthase, H^+ transporting, mitochondrial F1 complex, ε subunit	AF052955
20	*PDCD5*	Programmed cell death 5	AF014955
21	*CLPTM1L*	CLPTM1-like	AL137440
22	*PPP1R14B*	Protein phosphatase 1, regulatory (inhibitor) subunit 14B	X91195
23	*MRPL17*	Mitochondrial ribosomal protein L17	AK026857
24	*TUBA1B*	Tubulin, α1b	BC006481
25	*IFI6*	Interferon, α-inducible protein 6	X02492
26	*GAPDH*	Glyceraldehyde-3-phosphate dehydrogenase	AF261085
27	*SLC25A3*	Solute carrier family 25 (mitochondrial carrier; phosphate carrier), member 3	BC006455
28	*MAD2L2*	MAD2 mitotic arrest deficient-like 2 (yeast)	AF157482
29	*CTNNB1*	Catenin (cadherin-associated protein), β1, 88 kDa	X87838
30	*CALR*	Calreticulin	M84739
31	*MRPS6*	Mitochondrial ribosomal protein S6	BC000547
32	*ANGPTL2*	Angiopoietin-like 2	AF007150
33	*RPL38*	Ribosomal protein L38	Z26876
34	*ANAPC7*	Anaphase promoting complex subunit 7	AY007104
35	*ENO1*	Enolase 1, (α)	BC004325
36	*ALDH2*	Aldehyde dehydrogenase 2 family (mitochondrial)	M20456

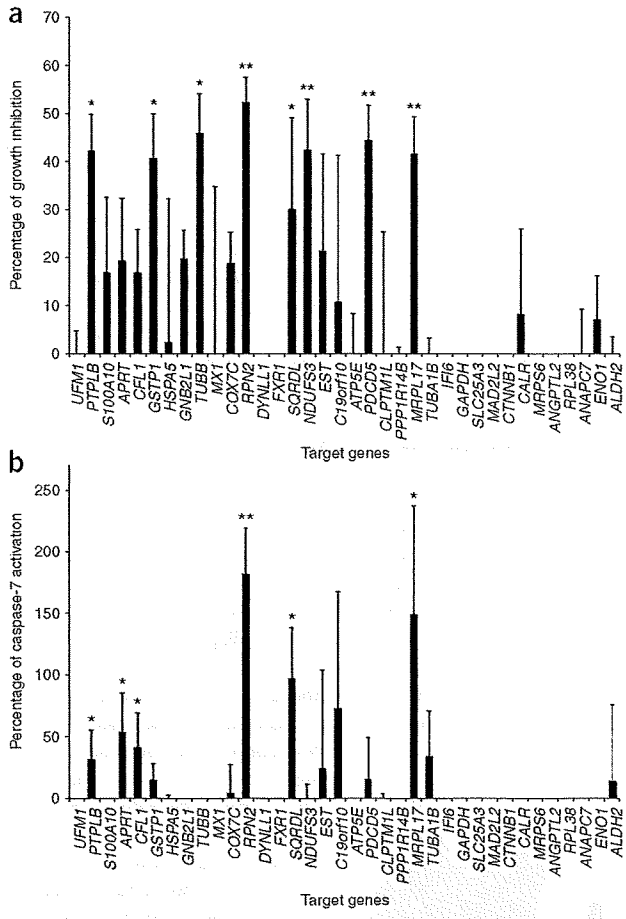

Figure 1 RNAi cell transfection array analysis in cultured breast cancer cells. **(a)** Inhibition of cell growth by 36 siRNAs on atelocollagen-based cell transfection arrays in the presence of docetaxel (1 nM) 72 h after transfection. The cell growth was estimated by luciferase activity in MCF7-ADR-Luc cells, which stably express luciferase ($n = 4$ per group; $^*P < 0.05$, $^{**}P < 0.01$). **(b)** Activation of caspase-7 by 36 siRNAs on atelocollagen-based cell transfection arrays in the presence of docetaxel (1 nM) 72 h after transfection. After the detection of luciferase activity, the same cell transfection arrays were assigned to the measurement of caspase-7 activity, which is elevated in apoptotic MCF7-ADR-Luc cells ($n = 4$ per group; $^*P < 0.05$, $^{**}P < 0.01$). Values are means ± s.d.

However, the expression of other genes was also found to correlate with docetaxel resistance by RNAi-based screening, and they could have some possible additive or synergistic effects with RPN2. Thus, we examined the induction of apoptosis after cotransfection of RPN2 siRNA and siRNAs against other genes that caused cell growth inhibition, apoptosis induction or both in docetaxel-resistant MC7-ADR cells. Knockdown of *PTPLB*, *APRT*, *CFL1*, *GSTP1*, *TUBB*, *SQRDL*, *NDUFS3*, *PDCD5* or *MRPL17* genes with simultaneous knockdown of *RPN2* did not significantly enhance caspase-7 activity relative to the knockdown of *RPN2* alone (**Supplementary Fig. 2b**). This result shows that knockdown of the other genes does not have an additive effect when used together with knockdown of RPN2.

We confirmed the efficacy of RPN2 siRNA for the knockdown of RPN2 messenger RNA by cell-direct real-time RT-PCR analysis. This analysis revealed that RPN2 siRNA inhibited 80% of the mRNA level relative to the control nontargeting siRNA (**Fig. 2d**). Immunofluorescence staining of the RPN2 protein revealed that the RPN2 protein localized in the cytoplasm and its expression was decreased by RPN2 siRNA (**Fig. 2e**). In further experiments, a liposome-mediated RPN2 siRNA transfection was performed. The western blot analysis showed a 45% reduction in RPN2 protein abundance (90% reduction of mRNA by real-time RT-PCR analysis) by RPN2 siRNA transfection in comparison with the control nontargeting siRNA (**Fig. 2f**). These results suggest that downregulation of RPN2 expression by siRNA inhibits cell growth and induces apoptosis in the presence of docetaxel.

In addition, we established stable clones expressing short hairpin RNA (shRNA) against RPN2 (shRNP2) and examined the effect on apoptosis induction in MCF7-ADR cells. The clone that expressed the lowest RPN2 mRNA level showed a 70% reduction of RPN2 expression relative to the control clone ($P < 0.001$, **Supplementary Fig. 2c**), and this shRPN2 clone showed a high caspase-7 activity as compared to the control clone in the presence of docetaxel ($P < 0.001$, **Supplementary Fig. 2d**). We examined seven independent clones and found that they all showed a similar phenotype of increasing drug sensitivity (data not shown). Therefore, consistent with our results with synthetic RPN2 siRNA, the data from the shRPN2 experiments provide evidence for the involvement of RPN2 in drug resistance.

To evaluate the effect of RPN2 siRNA on the drug response of MCF7-ADR cells, we measured the half-maximal inhibitory concentration (IC_{50}) for taxanes. The IC_{50} values for docetaxel in MCF7 and MCF7-ADR cells were 9.48 ± 1.48 nM and 40.22 ± 5.14 nM, respectively ($P < 0.001$). RPN2 siRNA–transfected MCF7-ADR cells were 3.5-fold more sensitive to docetaxel compared with nontargeting siRNA–transfected cells (IC_{50} of 11.47 ± 1.97 nM versus 39.48 ± 2.98 nM, $P < 0.001$). Thus, RPN2 silencing makes MCF7-ADR cells sensitive to docetaxel to a degree similar to that in drug-sensitive MCF7 cells. For paclitaxel, another taxane, the IC_{50} values in MCF7 and MCF7-ADR cells were 13.00 ± 2.02 nM and 89.74 ± 3.43 nM, respectively ($P < 0.001$). RPN2 siRNA–transfected MCF7-ADR cells were 2.6-fold more sensitive to paclitaxel compared with nontargeting siRNA–transfected cells (IC_{50} of 32.92 ± 3.89 nM versus 84.39 ± 5.48 nM, $P < 0.001$). These results indicate that RPN2 silencing bestows a hypersensitive response to taxanes to drug-resistant breast cancer cells.

In addition, we examined docetaxel-resistant EMT6/AR10.0 cells with high expression of the mouse *Rpn2* gene and the *Mdr1* (*Abcb1b*) and *Mdr3* (*Abcb1a*) genes, which reportedly have a similar role in drug resistance to that of the *MDR1* gene in humans, to see whether they have a similar phenotype to MCF7-ADR cells in terms of RPN2 expression status and drug resistance. The siRNA-mediated knockdown of mouse Rpn2 (70% reduction of mRNA by real-time RT-PCR analysis) significantly induced apoptosis of cells in the presence of docetaxel (**Supplementary Fig. 2e–g**). In contrast, nontargeting control siRNA showed no effect (**Supplementary Fig. 2e–g**). Therefore, these results suggest that RPN2 confers docetaxel resistance to both human and mouse cell lines.

Induction of RPN2 expression by docetaxel treatment

Real-time RT-PCR analysis showed that docetaxel-resistant MCF7-ADR cells expressed a slightly increased level of RPN2 mRNA (approximately 20%, $P < 0.01$) relative to parental MCF7 cells (**Fig. 3a**). However, RPN2 mRNA expression in parental MCF7 cells was markedly induced by docetaxel in a dose-dependent manner at

48 h after treatment (**Fig. 3b**). These data indicate that RPN2 mRNA induction may correlate with the observed antiapoptotic phenotype of MCF7-ADR cells.

Furthermore, MCF7-ADR cells expressed abundant MDR1 mRNA, which is a major cause of docetaxel resistance, whereas docetaxel-sensitive MCF7 cells did not (**Fig. 3c**). Additionally, MDR1 mRNA expression in MCF7 cells was strongly induced by docetaxel at 48 h after treatment (**Fig. 3d**). Together, these data provide a new insight into the development of docetaxel resistance in MCF7 cells: when breast cancer cells coordinately express a high amount the of *MDR1* and *RPN2* gene products, the cells become drug-resistant.

RPN2 expression associates with response to docetaxel

In this study, subjects with breast cancer with complete response and partial response were defined as responders, whereas subjects with no change and progressive disease were defined as nonresponders, in accordance with World Health Organization criteria[16] (**Supplementary Note** online).

Of the 44 subjects, 22 showed a pathologic response to docetaxel, and the other 22 showed no response[16]. To understand the clinical importance of the status of RPN2 expression in the subjects, we compared the expression level (signal log ratio) for RPN2 transcript between nonresponder and responder subjects by the Mann-Whitney *U*-test. The subjects with higher RPN2 expression showed a significantly lower response rate to docetaxel than did those with relatively low expression of RPN2 (signal log ratio expressed as mean ± s.e.m. in nonresponders was 0.347 ± 0.062 versus 0.111 ± 0.052 in responders; $P = 0.0052$). Thus, there is a significant association of RPN2 expression with the pathologic response to docetaxel. Although the data are not shown, RPN2 mRNA expression was significantly increased in cancerous tissues compared to that in normal tissues.

Furthermore, we also assessed validated sets of new samples from 26 subjects with breast tumors (12 responders and 14 nonresponders). The expression of RPN2 was higher in nonresponders than in responders (nonresponders, 0.240 ± 0.066, versus responders, 0.025 ± 0.194). Because of the small sample size in the validation set, we have not obtained conclusive results at this time. We are currently seeking larger samples that will be tested in the near future. However, when we combined studies with subjects in the learning and validation sets, RPN2 expression was significantly higher in nonresponders (34 subjects) than in responders (36 subjects) (nonresponders, 0.306 ± 0.046, versus responders, 0.080 ± 0.075; $P = 0.0219$).

Downregulation of RPN2 in orthotopic breast tumors

To extend our *in vitro* findings and to determine whether RPN2 could be an effective therapeutic target for docetaxel-resistant breast cancer, we examined the effect of RPN2 siRNA on an animal model of breast tumors by orthotopically implanting MCF7-ADR cells into mice and using an atelocollagen-mediated *in vivo* siRNA delivery[21,22]. We injected the RPN2 siRNA or nontargeting control siRNA (1 nmol per tumor) with 0.5% atelocollagen in a 200 µl volume into tumors that had reached 4–5 mm in diameter 7 d after inoculation of MCF7-ADR cells. At the time of siRNA administration, docetaxel was intraperitoneally (i.p.) injected into the mice. Subsequent tumor development was monitored by measuring the tumor size for a week. Mice that had been administered the RPN2 siRNA–atelocollagen complex and docetaxel (20 mg kg^{-1} i.p.) showed a significant decrease in tumor size (mean ± s.d.; day 0, 52 ± 8 mm^3; day 7, 21 ± 8 mm^3) relative to mice that had been administered the control nontargeting siRNA–atelocollagen (day 0, 37 ± 7 mm^3; day 7, 35 ± 12 mm^3; $P < 0.01$) (**Fig. 4a**). The tumor size was markedly reduced by administration of RPN2 siRNA with docetaxel at 7 d after treatment (**Fig. 4b**). In the absence of docetaxel, RPN2 siRNA treatment slightly reduced MCF7-ADR tumor size relative to controls; however, there were no statistically significant differences (**Supplementary Fig. 3a** online). We also observed that docetaxel alone had no significant effect on tumor growth (**Supplementary Fig. 3a**). Furthermore, no significant differences were observed in tumor growth between mice treated with control nontargeting siRNA and untreated mice in the presence or in the absence of docetaxel (data not shown). Thus, RPN2 siRNA is useful for reducing the size of orthotopic MCF7-ADR breast tumors in the presence of docetaxel. Additionally, to evaluate the effect of sustained treatment with siRNA, we treated mice with tumors twice by injection of siRNA-atelocollagen complex. RPN2 siRNA or nontargeting control siRNA (1 nmol per tumor) were injected into the tumors (diameter, 4 mm) at days 0

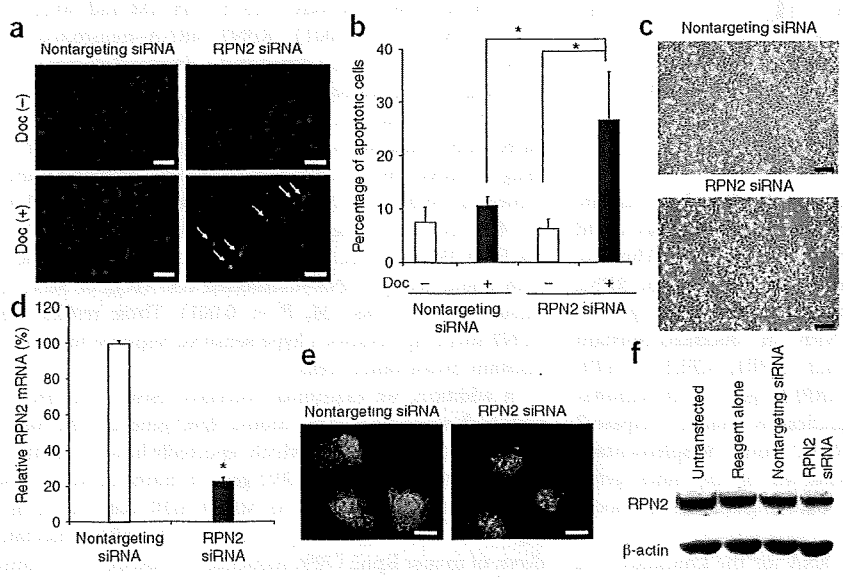

Figure 2 Apoptosis of MCF7-ADR cells transduced with RPN2 siRNA. **(a)** Hoechst staining of cells in the presence or absence of docetaxel (Doc, 1 nM) 72 h after the transfection of RPN2 siRNA. Scale bar, 50 µm. The arrows indicate cells with nuclear condensation and fragmentation. **(b)** Numbers of apoptotic cells from **a**. The data show the percentage of apoptotic cells in the presence or absence of docetaxel (1 nM) 72 h after the transfection of RPN2 siRNA. As a control, nontargeting control siRNA was used ($n = 4$ per group, $^*P < 0.02$). **(c)** Phase-contrast micrograph of MCF7-ADR cells 72 h after treatment with RPN2 siRNAs or control nontargeting siRNAs in the presence of docetaxel. Scale bar, 200 µm. **(d)** Knockdown of RPN2 mRNA by RPN2 siRNA in a cell transfection array, as monitored by cell-direct real-time RT-PCR analysis. As a control, nontargeting siRNA was used ($n = 4$ per group, $^*P < 0.001$). **(e)** Immunofluorescence staining of the RPN2 protein in MCF7-ADR cells 72 h after treatment with RPN2 siRNAs or control nontargeting siRNAs. Scale bar, 5 µm. **(f)** Western blot analysis of RPN2 protein in MCF7-ADR cells treated with RPN2 siRNAs or control nontargeting siRNAs 72 h after the liposome-mediated transfection. Values are means ± s.d.

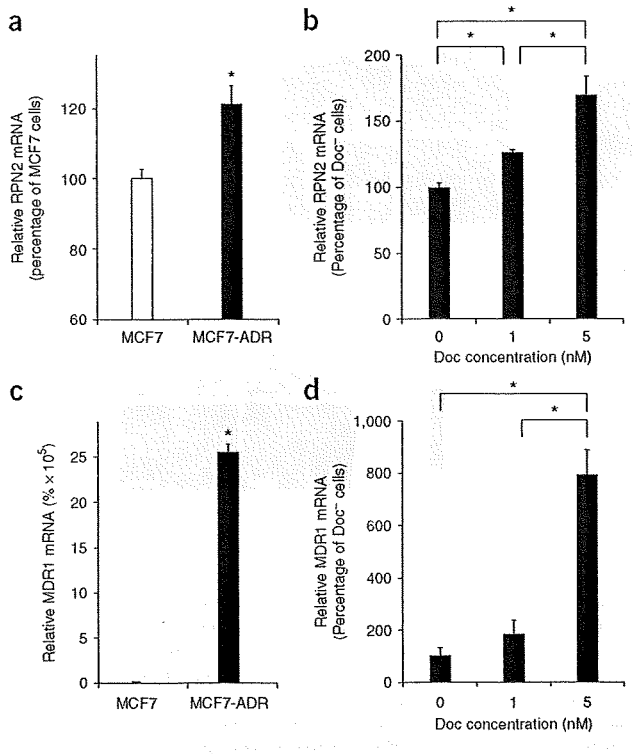

Figure 3 Induction of RPN2 and MDR1 expression by docetaxel treatment. RPN2 mRNA and MDR1 mRNA expression were analyzed by real-time RT-PCR. **(a)** RPN2 expression in drug-resistant MCF7-ADR cells and parental drug-sensitive MCF7 cells ($n = 3$ per group, $^*P < 0.01$). **(b)** Expression of RPN2 induced by docetaxel treatment in parental MCF7 cells. The data shown are from 48 h after the treatment ($n = 3$ per group, $^*P < 0.01$). **(c)** MDR1 expression in drug-resistant MCF7-ADR cells and parental drug-sensitive MCF7 cells ($n = 3$ per group, $^*P < 0.001$). The numbers on the *y* axis represent percentage ($\times 10^5$) of MCF7 cells. **(d)** Expression of MDR1 induced by docetaxel treatment in parental MCF7 cells. The data shown are from 48 h after the treatment ($n = 3$ per group, $^*P < 0.01$). Values are means ± s.d.

and 10. Simultaneously, docetaxel (20 mg kg^{-1} i.p.) was injected into the mice. We observed the mice for 20 d. Mice that had been given RPN2 siRNA and docetaxel showed significantly suppressed tumor growth relative to the mice that were administered control nontargeting siRNA at day 20 after the treatment ($P < 0.05$, **Supplementary Fig. 3b,c**). Mice showed no toxic effect during the observation period.

Furthermore, we examined the effect of RPN2 siRNA on a second animal model of breast tumors by orthotopically implanting MDA-MB-231/MDR1 cells. First, we established an MDA-MB-231/MDR1 cell line, which expresses the *MDR1* gene inducing docetaxel resistance. In this study, MDR1 expression is a key factor, because we are proposing that the coordinate expressions of RPN2 and P-glycoprotein may participate in the mechanism of docetaxel resistance. We injected the RPN2 siRNA or nontargeting control siRNA (2 nmol per tumor) with 0.5% atelocollagen in a 200 µl volume into tumors that were 5–6 mm in diameter 8 d after inoculation of MDA-MB-231/MDR1 cells. At the same time of siRNA administration, we injected docetaxel i.p. into the mice. Because docetaxel at a dose of 20 mg kg^{-1} in mice slightly suppressed MDA-MB-231/MDR1 tumor growth, we reduced the dose of docetaxel to 7 mg kg^{-1}, corresponding to the IC_{50} value of docetaxel in MDA-MB-231/MDR1 cells, which was 35% of that of MCF7-ADR cells. At a dose of 7 mg kg^{-1} docetaxel, mice treated with docetaxel alone showed no significant change in tumor growth. Subsequent tumor development was monitored by measuring the tumor size for a week. Mice that had been administered the RPN2 siRNA–atelocollagen complex and docetaxel (7 mg kg^{-1} i.p.) showed a significant inhibition of tumor growth (day 0, 61 ± 21 mm^3; day 7, 97 ± 24 mm^3) relative to mice that had been administered the control nontargeting siRNA–atelocollagen complex (day 0, 68 ± 9 mm^3; day 7, 154 ± 23 mm^3) (**Fig. 4c,d**). The value was statistically significant, with $P < 0.002$. Tumors treated with RPN2 siRNA in the absence of docetaxel showed no significant inhibition relative to control tumors that had been given nontargeting siRNA or docetaxel alone (data not shown). These results show that the growth of docetaxel-resistant MDA-MB-231/MDR1 tumors was suppressed by administration of RPN2 siRNA and docetaxel. Thus, RPN2 silencing is effective for the suppression of tumor growth in two models for docetaxel-resistant breast cancer in the presence of docetaxel.

RPN2 siRNA delivery augments docetaxel-induced apoptosis

MCF7-ADR tumors treated with RPN2 siRNA were investigated for apoptotic activity after docetaxel treatment for 3 d. TUNEL staining of tumor tissue treated with RPN2 siRNA revealed a significant number of apoptotic cells relative to the number in nontargeting control siRNA–treated tumors ($P < 0.01$, **Fig. 4e,f**). In contrast, RPN2 siRNA–transduced tumors in the absence of docetaxel showed no marked apoptotic cell death (**Fig. 4e,f**). We have also previously shown that atelocollagen alone does not induce any cytotoxic or inflammatory effect when it is injected into mice[23,24]. In a subsequent experiment, the mRNA levels of RPN2 in treated tumors were measured. RPN2 expression was significantly reduced in mouse tumors after combined treatment with RPN2 siRNA and docetaxel ($P < 0.05$, **Fig. 4g**). Furthermore, the RPN2 protein abundance in treated tumors was markedly downregulated by RPN2 siRNA (**Fig. 4h**). Thus, these results altogether indicate that RPN2 siRNA induces tumor inhibition via augmentation of docetaxel-induced apoptotic cell death *in vivo*.

To examine docetaxel retention in the tumors in the *in vivo* experiment, we performed drug disposition analysis. Eleven hours after docetaxel administration, we dissected the tumors and determined the amount of docetaxel incorporated into the tumors by HPLC with ultraviolet detection at 225 nm after solid-liquid extraction. We detected docetaxel in tumors that had received RPN2 siRNA ($n = 4$) at a range of 667 to 1400 ng per wet gram of tissue (**Fig. 4i**). In contrast, the tumors that received control siRNA ($n = 4$) showed a very low amount of docetaxel (~10 ng per wet gram of tissue). Thus, the results clearly indicate that abrogation of RPN2 expression in drug-resistant tumors results in docetaxel accumulation in those tumors.

RPN2 siRNA reduces *N*-linked glycosylation of MDR1

The mammalian *RPN2* gene encodes a type I integral membrane protein found only in the rough endoplasmic reticulum[25,26]. The RPN2 protein is part of an *N*-oligosaccharyl transferase complex that links high mannose oligosaccharides to asparagine residues found in the N-X-S/T consensus motif of nascent polypeptide chains[27]. The expression of the multidrug transporter P-glycoprotein, encoded by *MDR1*, is one of the causes of clinical drug resistance to taxanes. Real-time RT-PCR analysis showed that MCF7-ADR cells expressed abundant MDR1 mRNA, whereas parental cells did not (**Fig. 3c**). In addition, the MDR1 mRNA amount was not significantly decreased

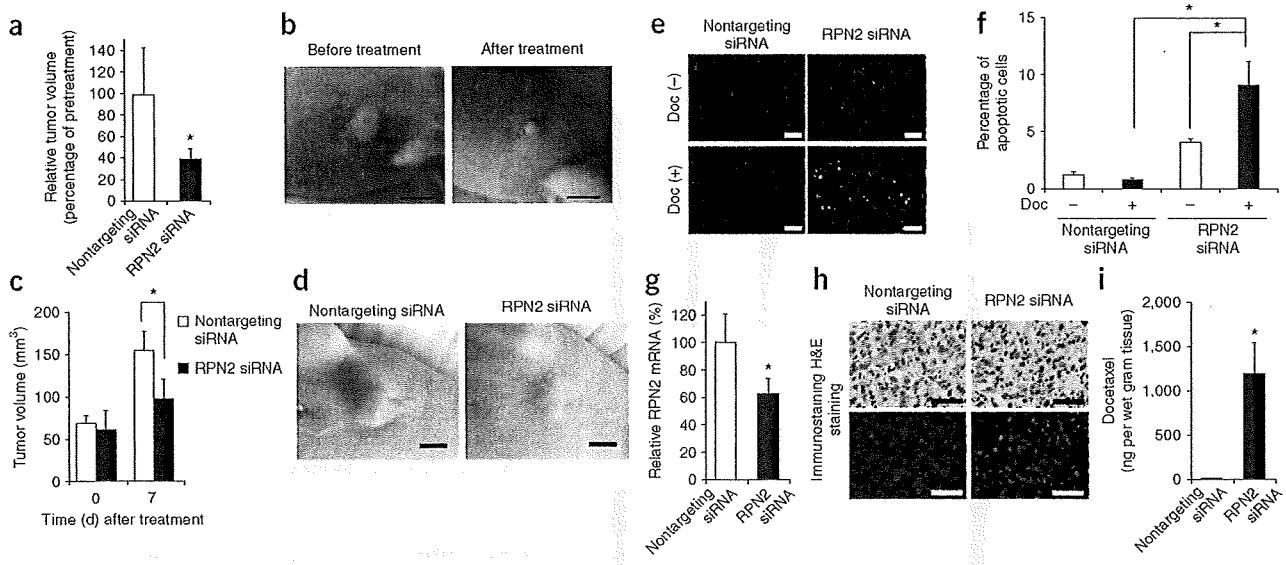

Figure 4 Delivery of RPN2 siRNA to docetaxel-resistant breast tumors. The effect of RPN2 siRNA was examined in orthotopic breast tumor models. **(a)** Reduction of MCF7-ADR breast tumor volume in mice given RPN2 siRNA or control nontargeting siRNA along with docetaxel ($n = 6$ per group, $^*P < 0.01$). **(b)** siRNA-treated MCF7-ADR tumors in mice before and 7 d after docetaxel treatment. Scale bar, 5 mm. **(c)** Growth of MDA-MB-231/MDR1 breast tumor in mice administered RPN2 siRNA or nontargeting siRNA along with docetaxel ($n = 6$ per group, $^*P < 0.002$). **(d)** MDA-MB-231/MDR1 tumors in mice 7 d after treatment with siRNA and docetaxel. Scale bar, 5 mm. **(e)** TUNEL staining of MCF7-ADR tumor tissues treated with RPN2 siRNAs or nontargeting siRNAs in the presence or absence of docetaxel. Scale bar, 50 μm. **(f)** TUNEL-positive cells were counted and are represented in the graph ($n = 3$ per group, $^*P < 0.01$). **(g)** Expression of RPN2 mRNA in MCF7-ADR tumors treated with RPN2 siRNAs or nontargeting siRNAs ($n = 3$ per group, $^*P < 0.01$). **(h)** Expression of RPN2 protein in MCF7-ADR tumors. H&E staining and RPN2 immunofluorescence staining (green, RPN2; blue, nuclei) of tissues treated with RPN2 siRNA or nontargeting siRNA. Scale bar, 50 μm. **(i)** Docetaxel retention in MCF7-ADR tumors in mice treated with RPN2 siRNAs or nontargeting siRNAs ($n = 4$ per group, $^*P < 0.001$). Values are means ± s.d.

in MCF7-ADR cells transduced by RPN2 siRNA (**Supplementary Fig. 4** online). For this reason, and to assess the potential involvement of *RPN2* gene overexpression in MDR1 functions, we tested the glycosylation status of MDR1 protein in MCF7-ADR cells transfected with RPN2 siRNA. We analyzed the glycosylation patterns by western blotting of P-glycoprotein, which appears on blots as mature 170-kDa, immature (partially glycosylated) 150-kDa and unglycosylated 140-kDa bands[28]. The 150-kDa immature and 140-kDa unglycosylated P-glycoproteins were clearly found in MCF7-ADR cells with RPN2 knockdown (90% inhibition of mRNA by real-time RT-PCR analysis; **Fig. 5a**). More than 80% of P-glycoproteins were unglycosylated or partially glycosylated in RPN2-silenced cells (composition of P-glycoproteins, 170 kDa:150 kDa:140 kDa = 18:40:42). In contrast, MCF7-ADR cells transduced with nontargeting control siRNA expressed more than half of their P-glycoproteins as170-kDa mature P-glycoprotein (170 kDa:150 kDa:140 kDa = 52:17:31). This result showed that RPN2 knockdown inhibits glycosylation of P-glycoproteins in MCF7-ADR cells. The western blot of P-glycoprotein, particularly in cells transduced with RPN2 siRNA, showed 'smear' patterns (**Fig. 5a**). We speculated that the smear pattern was caused by the presence of intermediately glycosylated forms in various sizes. We treated the cell lysate samples with peptide:*N*-glycosidase F (PNGase F) to remove *N*-glycan chains, which shifted the P-glycoprotein in the blot from a smear pattern to a 140-kDa unglycosylated protein band in MCF7-ADR cell lysates. After PNGase F treatment, both nontargeting control siRNA– and RPN2 siRNA–transduced cells showed a 140-kDa unglycosylated P-glycoprotein band (**Fig. 5a**). This indicates that the smear pattern resulted from the presence of intermediately glycosylated P-glycoprotein and that there were a number of intermediately glycosylated P-glycoproteins in the RPN2-silenced cells because of inhibition of glycosylation on P-glycoprotein.

We further evaluated the RPN2 siRNA effects on cell surface P-glycoprotein expression in MCF7-ADR cells by immunofluorescence staining. As expected, immunofluorescence staining indicated that P-glycoprotein was predominantly localized to the cell membrane in MCF7-ADR cells transduced with control nontargeting siRNAs, whereas the intensity of membrane P-glycoprotein in RPN2-downregulated cells was considerably reduced (**Fig. 5b**). Moreover, retention of rhodamine-123, which is a substrate of P-glycoprotein, was strongly enhanced in MCF7-ADR cells transfected with RPN2 siRNA compared to those transfected with nontargeting siRNA (**Fig. 5c**). This indicates that downregulation of RPN2 restores drug retention and inhibits P-glycoprotein function by suppressing the glycosylation of P-glycoproteins in MCF7-ADR cells.

To further bolster these findings, we performed immunostaining analysis of RPN2 and P-glycoprotein in MCF7-ADR tumors in mice. The RPN2 shutdown resulted in a marked disappearance of the membrane-bound P-glycoprotein (**Fig. 5d**), an observation that supports our *in vitro* findings that RPN2 downregulation by siRNA in drug-resistant MCF7-ADR cells results in the loss of membrane-bound P-glycoprotein.

Furthermore, we have examined the status of RPN2 and P-glycoprotein in breast cancer tissues from subjects with RPN2 mRNA high expression ($n = 4$) and RPN2 mRNA low expression ($n = 4$) by immunostaining. P-glycoprotein was predominantly localized to the cell membrane in the primary tumor with a strong signal for RPN2, whereas in the primary tumor with low expression of RPN2, P-glycoprotein was found in the cytoplasm (**Supplementary**